frontiers | Frontiers in Earth Science

TYPE Original Research
PUBLISHED 03 April 2025
DOI 10.3389/feart.2025.1484909

Check for updates

OPEN ACCESS

EDITED BY
Davide Gamboa,
University of Aveiro, Portugal

REVIEWED BY
Murat Gül,
Mugla University, Türkiye
Sheng Fu,
Xi'an Shiyou University, China
Keji Yang,
Hebei GEO University, China
Omar A. M. Mohammad,
University of Kirkuk, Iraq

*CORRESPONDENCE
Bingshan Ma,
mabingshan09@163.com

RECEIVED 22 August 2024
ACCEPTED 09 January 2025
PUBLISHED 03 April 2025

CITATION
Dong H, Ma B, Wan X, Liang J, Liang B, Zhang Q, Zhang M and Mo G (2025) Characteristics and evolutionary process of low-mature paleo-subsurface rivers in carbonate sequences and controls on hydrocarbon accumulation in the northern Tarim Basin, NW China.
Front. Earth Sci. 13:1484909.
doi: 10.3389/feart.2025.1484909

Characteristics and evolutionary process of low-mature paleo-subsurface rivers in carbonate sequences and controls on hydrocarbon accumulation in the northern Tarim Basin, NW China

Hongqi Dong[1,2,3], Bingshan Ma[4]*, Xiaoguo Wan[5], Jiapeng Liang[1,2], Bin Liang[1,2], Qingyu Zhang[1,2], Meng Zhang[1,2] and Guochen Mo[1,2]

[1]CAS/Key Laboratory of Karst Dynamics, Institute of Karst Geology, Ministry of Nature Resources (MNR), International Research Centre on Karst under the Auspices of UNESCO, Guilin, Guangxi, China, [2]Pingguo Guangxi, Karst Ecosystem, National Observation and Research Station, Pingguo, Guangxi, China, [3]School of Environmental Studies, China University of Geosciences, Wuhan, China, [4]School of Geoscience and Technology, Southwest Petroleum University, Chengdu, China, [5]PetroChina Tarim Oilfield Company, Korla, China

Paleo-subsurface rivers can serve as high-quality reservoir spaces for hydrocarbon accumulation within the carbonate sequence stratigraphy. However, the characteristics and evolutionary process of the typical low-mature paleo-subsurface rivers are rarely discussed, constraining petroleum exploration and exploitation. This study employs an integrated approach, combining seismic-geological analysis, core and thin sections, logging data, and production data within paleo-subsurface rivers to investigate the structural features and evolutionary processes of the paleo-subsurface river in the Halahatang area of the Tarim Basin, and further discuss their implications for reservoir development and hydrocarbon accumulation. The findings reveal: 1) Low-maturity paleo-subsurface rivers predominantly exhibit partially throughgoing characteristics, displaying a spatially discontinuous, downward-dipping pattern. 2) The evolutionary process of these paleo-subsurface rivers can be categorized into four distinct stages: initial isolated stage, expanded and partially through-going stage, nearly through-going stage, and condensed and partially throughgoing stage. 3) The evolution of the subsurface rivers has resulted in the segmented reservoirs, which consequently influence the compartmentalized accumulation and entrapment of hydrocarbons. The characteristics of the partially through-going subsurface rivers and their associated oil and gas reservoirs in the Halahatang area provide valuable insights for exploration and exploitation of ultra-deep carbonate reservoirs.

KEYWORDS

paleo-subsurface river, low-mature, partially through-going, evolutionary process, carbonate sequence, Tarim Basin

1 Introduction

Subsurface river systems are typically formed through prolonged dissolution and scouring processes by groundwater in soluble rocks, primarily limestone and dolomite (Ren and Liu, 1983; Wang, 2010; Yuan, 1993). These systems can exist as independent entities or as integral components of comprehensive groundwater networks, exhibiting diverse geometries influenced by tectonic settings, lithological variations, and hydrological conditions (Ford and Williams, 2007). Common morphological types include single-tube (Palmer, 2007; 2011), branching (Ford and Williams, 2007), network, vug-cave (Audra et al., 2010; Palmer, 2007; 2011), tunnel (Klimchouk et al., 2016) types. The subsurface river systems often develop in fluvial, deltaic, or glacial depositional environments, with their morphology influenced by tectonic activity, sediment supply, and climatic conditions. Advanced geophysical techniques, such as 3D seismic imaging and sedimentological analysis, have been pivotal in reconstructing their paleochannel architectures. Subsurface river system plays a significant role in the hydrological cycle (Ford and Williams, 2007), CO_2 cycle (Xie et al., 2024), biodiversity conservation (Culver and Pipan, 2019), climate change (Panneerselvam et al., 2022), and so on. Paleo-subsurface rivers, formed during previous geological periods and subsequently buried through sedimentation, tectonic activities, or other geological processes (Miall, 1996), providing insights for stratigraphic analysis (Reading and Richards, 1994), paleoclimatology and environmental reconstruction (Dong et al., 2024), especially, it provides the reservoir space for preserving the evolution of fluids and the storage of mineral resources, including petroleum reserves (Huang and Song, 1997; Gao et al., 2016; Wu et al., 2018a; Zhong et al., 2018; Zhang et al., 2020a).

Over the past decades, petroleum exploration and exploitation results have proved that the paleo-subsurface rivers play an essential role in oil and gas resources by controlling the reservoir and hydrocarbon accumulation (Loucks and Mescher, 2004). Key findings indicate that subsurface rivers serve as high-quality reservoirs due to their porosity and permeability, often acting as conduits or traps for hydrocarbons. Recent research highlights the importance of understanding stratigraphic stacking patterns and incision-fill dynamics, which control reservoir heterogeneity and connectivity and further influence hydrocarbon migration and accumulation. The identification and characterization of paleo-subsurface rivers have been greatly enhanced through the application of advanced methodologies, including seismic interpretation-based paleo-geomorphological method (Burberry et al., 2016; Xiong et al., 2021), core and thin section observation for recognizing architecture (Dong et al., 2024), and geochemical method (Onac, 2014; Polyak et al., 2014) were separately or comprehensively utilized to analysis the geometry (Zhang et al., 2021), collapse-infilling characteristics (Loucks and Mescher, 2002; Dong et al., 2024), karst stages (Arosi and Wilson, 2015; Dong et al., 2023), and influence on reservoirs (Smith, 2006; Davies and Smith, 2006) in the paleo-subsurface river system. However, these researches primarily focus on large-scale and nearly through-going paleo-subsurface rivers, i.e., those in the mature evolutionary process. In contrast, the characteristics, mechanisms, and contributions to reservoir formation and hydrocarbon accumulation of small-scale and partial through-going (low-mature) paleo-subsurface rivers are rarely discussed.

The Halahatang area, located on the slope of the northern uplift in the Tarim Basin, displays a distinct north-to-south zonation of karst features, comprising the buried-hill karst zone, inter-bedded karst zone, and fault-controlled karst zone (Zhang, 2018). Seismic imaging and drilling data have confirmed the presence of a small-scale paleo-subsurface river system in this area (Jiang and Li, 2021). While exploration activities have identified associated oil and gas reservoirs, the tectonic setting, karst characteristics, and structural features of this paleo-subsurface river system differ significantly from the mature, multi-phase infilling patterns observed in the Tahe Oilfield (Ding et al., 2020; Ning et al., 2021; Chen et al., 2023; Xia and Liang, 2011; Yang et al., 2023). The formation mechanisms and controlling factors of this small-scale paleo-subsurface river system remain subjects of ongoing debate, and its impact on hydrocarbon accumulation processes is not yet fully understood, necessitating further investigation.

This study employs an integrated approach, combining seismic geological interpretation, core and thin section analysis, and single-well log evaluation, to systematically investigate the architectural characteristics and evolutionary processes of paleo-subsurface rivers in the Halahatang area. The research focuses on elucidating the mechanisms controlling reservoir formation and hydrocarbon accumulation within these systems. The findings are expected to provide valuable insights and potential exploration strategies for carbonate karst reservoirs in deep slope environments, thereby contributing to the advancement of hydrocarbon exploration in complex geological settings.

2 Geological setting

2.1 Location and tectonic evolution

The Tarim Basin covers an area of 560,000 km^2, and it is the largest oil- and gas-bearing basin in China, which is located between the northern Tianshan Mountain and the Southern Kunlun-Altun Mountains (Zhang et al., 2022a) (Figure 1A). The basin contains the Late Neoproterozoic–Quaternary sediments covering Archean–Early Neoproterozoic crystalline basement with

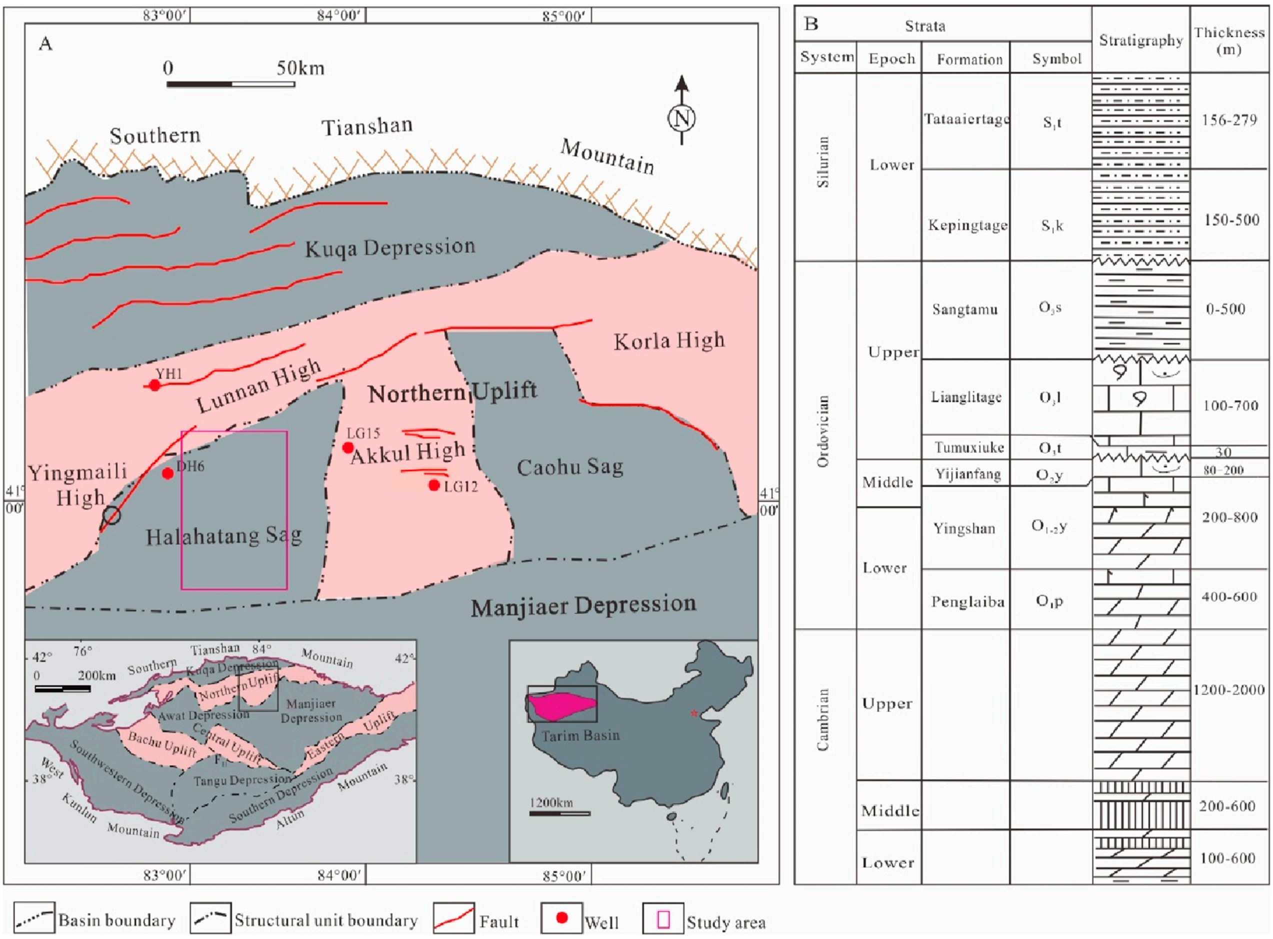

FIGURE 1
Simplified map of the tectonic units **(A)** and comprehensive stratigraphic column in the northern Tarim Basin **(B)** (after Dong et al., 2024).

a thickness of more than 10 km (Xu and Ma, 2022) (Figure 1B). The Northern Uplift (or Tabei Uplift) is a pre-Jurassic uplift, between the Kuqa and the Majiaer depressions. The study area is located on the southern slope of the Northern Uplift of the Tarim Basin (Figure 1A). The study area experienced multi-stage tectonic movement from the Cambrian to Neogene (Tang et al., 2019; Jia, 1997; Xu et al., 2022; Zhao et al., 2023). The intra-platform uplift belt gradually formed and the carbonate platform developed during the Cambrian to Mid-Ordovician. During the middle to late Ordovician, a large south-dipping slope was formed in the Lunnan area (Ma and Duan, 2023). During the Silurian to Devonian, the Lunnan Uplift continuously uplifted and the Halahatang nose structure began to form (Wu et al., 2020; Ma et al., 2022; Ma et al., 2024). Since the Neogene, the Kuqa Depression has been strongly subsiding and the Lunnan Uplift was finally formed. In addition, the study area is predominantly characterized by the development of an X-shaped conjugate strike-slip fault system (Wu et al., 2016; Wu et al., 2020; Zhao et al., 2023; Ma et al., 2024), which was formed during the Middle Caledonian period and experienced multi-stage activation during the Carboniferous-Permian and Cenozoic (Wu et al., 2020; Ma et al., 2024).

2.2 Stratigraphy evolution and karst development

The Ordovician strata in the study area can be divided into the Penglaiba (O_1p), Yingshan (O_1y), Yijianfang (O_2y), Tumuxiuke (O_3t), Lianglitage (O_3l) and Sangtamu (O_3s) formations from bottom to top. The Middle-Lower Ordovician strata in the area are composed of a set of carbonate rocks formed in the platform facies (Jia et al., 2021; Liu et al., 2023; Wang et al., 2021). The stratigraphic architecture of the Ordovician sequence, spanning from the Sangtamu Formation to the Yingshan Formation, demonstrates a complex spatial distribution pattern characterized by progressive truncation, differential denudation, and lateral pinch-out along the south-north transect. The Lianglitage, Yijianfang, and Yingshan formations constitute the principal carbonate reservoir units within the study area, demonstrating a significant genetic relationship with strike-slip fault systems and karstification processes (Lin et al., 2021; Zhang et al., 2022b; Xu and Ma, 2022; Jia et al., 2021; Liu et al., 2023; Zhu et al., 2021). The Yingshan and Yijianfang formations were formed in the open platform facies with different lithology, the former includes sparry arenite, arenite micritic, and micritic limestone, and the latter is composed of bioclasts, sand clasts, micrite and oolitic limestones (Zhang et al., 2023; Zhao et al., 2023). The Yingshan Formation has been stratigraphically subdivided into four distinct members, with the first member occupying the uppermost position within the formation. The Tumuxiuke Formation comprises dense marl deposits characteristic of a subsiding platform facies, indicative of deposition in a progressively sinking platform environment. The Lianglitage Formation is predominantly characterized by platform margin facies, with carbonate sediments exhibiting significant spatial variations in composition and texture across different depositional environments (Zhao et al., 2023).

The study area has experienced multi-phase tectonic uplift accompanied by recurrent karstification events, resulting in the development of fracture-cavity systems within Ordovician carbonate rocks that exhibit multi-stage evolution and diverse filling patterns (Wu et al., 2018b; Wu et al., 2012a; Lin et al., 2021). The Ordovician carbonate rocks in the study area have undergone four distinct stages of exposure and weathering-related karstification, corresponding to a four-phase tectonic-sedimentary evolutionary process (Wu et al., 2012b; Ma and Duan, 2023; Chen et al., 2024). 1) Following the deposition of the Yijianfang Formation, the study area underwent tectonic uplift and subsequent denudation, accompanied by brief periods of weathering and karstification. 2) Subsequent to the Lianglitage Formation deposition, the region experienced renewed exposure, developing a distinct structural configuration characterized by elevated topography in the north and lower relief in the south. 3) Prior to the Silurian, partial stratigraphic denudation occurred, resulting in the direct exposure of several formations, including the Yijianfang and Yingshan formations, which collectively formed a pre-Silurian buried hill structure. 4) During the early Hercynian orogeny, intense folding of the northern orogenic belt led to the development of a localized unconformity between the Mid-Lower Ordovician strata and the overlying sedimentary sequences.

The Halahatang area, having undergone multiple phases of tectonic uplift, erosional denudation, and karstification, demonstrates pronounced zonal differentiation along the north-south transect (Li et al., 2015; Ma et al., 2019). The area can be systematically categorized into three distinct karst zones: a buried-hill karst zone, an inter-bedded karst zone, and a fault-controlled karst zone, each characterized by unique karstification processes and developmental patterns (Li, 2020; Ma et al., 2019; Zhang, 2018). The paleo-subsurface river systems are predominantly developed within the buried-hill karst zone and inter-bedded karst zone, where tectonically influenced karstification processes have generated a distinctive slope karst geomorphological configuration (Zhang et al., 2024; Jiang and Li, 2021). After multi-stage dissolution and transformation, a series of highly heterogeneous karst reservoir spaces such as paleo-subsurface rivers, large karst caves, and dissolution caves have been formed in the Yijianfang and Yingshan formations (Feng et al., 2023). The fracture-cavity reservoirs were further formed by the comprehensive influence of multi-stage faulting and karstification (Zhao et al., 2023).

3 Data and methodology

3.1 Paleotopography restoration

Three important tectonic-sedimentary hiatuses (i.e., O_2y-O_3t, O_3l-O3s, O_3s-S) were documented through sequence analysis using a drilling well and seismic data. An extensive dataset comprising over 5,000 km^2 of 3D prestack depth-migrated seismic reflection data was utilized for comprehensive horizon mapping and structural interpretation. Different paleogeographic restoration methods were applied to various stratigraphic levels based on the integration of distinct tectonic environments and lithological characteristics (Peng et al., 2009; Zhu et al., 2011; Dan et al., 2016; Wang et al., 2013; Zuo, 2019). Considering the distribution characteristics of the overlying and underlying strata, and the features of sedimentary hiatus, the paleo-geography of pre-Silurian were restored by the impression method. Through comprehensive thickness analysis spanning from the base of the Silurian Tataertag Formation to the top of the Ordovician sequence, paleo-thickness restoration was performed using compaction correction techniques. This enabled the construction of a thickness contour map delineating the interval from the Tataertag Formation base to the Ordovician top in the Halahatang area, effectively representing the pre-Silurian paleo geomorphological configuration of the region. The paleo-geography of the period of the Lianglitage Formation can be reconstructed by combining the remaining thickness with the paleo-structural trend surface of the strata. By utilizing structural data from the base of the Tataertag Formation to the base of the Tumuxiuke Formation, the structural trend surface of the top of the Yijianfang Formation during the pre-Silurian period was reconstructed. Structural data from the base of the Tataertag Formation to the top of the Ordovician were used to rebuild the structural trend surface of the top of the Ordovician during the pre-Silurian period. The paleo-structural trend surface of the top of the Yijianfang Formation was then restored by calculating the difference between the structural trend surface data of the top of the Ordovician and that of the top of the Yijianfang Formation during the pre-Silurian period. Using structural data from the base of the Sangtamu Formation to the base of the Tumuxiuke Formation, the residual thickness from the Lianglitage Formation to the top of the Yijianfang Formation was calculated. Finally, by integrating the residual thickness with the paleo-structural trend surface, the paleokarst geomorphology of the top of the Lianglitage Formation was restored. The paleo-geography of the period of the Yijiangfang Formation can be reconstructed by a combination method of the residual thickness method and residual thickness trend surface method. The residual thickness and residual thickness trend surface integration method involves the following steps: Utilizing the thickness (residual thickness) from the base of the Yingshan Formation's second member or the Penglai Formation's base to the depositional hiatus surface and calculating the residual between the residual thickness trend surface data and the residual thickness data. Constructing the residual thickness trend surface and its mirrored surface and restoring the paleokarst geomorphology of the depositional hiatus surface at the top of the Yijianfang Formation by integrating the mirrored residual thickness trend surface with the residuals.

3.2 Seismic-logging-core-based integrated identification method of paleo-subsurface rivers

Subsurface river systems typically reserve a more significant amount of void space, or are filled with low-velocity lithologies, resulting in seismic velocities within the subsurface river strata that are significantly lower than those of the surrounding dense limestones (Gao et al., 2016). Consequently, they often exhibit strong reflective seismic characteristics on seismic profiles, typically manifesting as strong amplitude, which is markedly different from the surrounding rocks (Burberry et al., 2016). Due to the complex structure and diverse fill materials of the subsurface river, chaotic point-like strong reflections and chaotic point-like weak reflections may also be the seismic response of the paleo-river. The former appears on the seismic profile as multiple point-like strong reflections distributed chaotically in the vertical direction, with planar attributes along a line, which may indicate multi-layered cave structures; the latter appears as chaotic weak reflections on the seismic profile, with a disordered occurrence and no distinct features, only slightly enhanced amplitude compared to the surrounding rocks, possibly indicating small-scale fracture-cavity volumes. Tensor attributes can, to a certain extent, reflect the variations of seismic characteristics and further indicate the locations of fracture-cavity systems, which have already demonstrated significant value in hydrocarbon exploration. From the logging curves, the position where the subsurface river is encountered shows characteristics of high gamma, low resistivity, low density, and high acoustic transit time, and there may also be phenomena of gas leakage. Differences in the internal fill structure of the paleo-river can also be directly observed on imaging logs and cores.

3.3 Geochemical method for fillings analysis

A total of 33 samples were collected from the Yijianfang Formation of the Middle Ordovician strata, which is comprised of calcite, mud, and siliceous clasts. The samples underwent sequential pretreatment processes following standardized protocols, including grinding, drying, and acidification. Carbon and oxygen isotope analyses were conducted using a stable isotope ratio mass spectrometer (Model: MAT253, Thermo Fisher Scientific, Waltham, MA, United States) at the Karst Geological Resources and Environmental Supervision and Inspection Center of the Ministry of Natural Resources. The instrument demonstrated a precision of 0.1‰ for both $\delta^{13}C$ and $\delta^{18}O$ determinations. All analyses were performed under controlled laboratory conditions, maintaining an ambient temperature of 24.3°C and relative humidity of 40% to ensure measurement consistency and reliability.

4 Results

4.1 Seismic-geological characteristics of paleo-subsurface rivers

Paleo-topographic reconstruction analysis revealed the presence of 9 major surface rivers, totaling approximately 241.76 km in length, and 28 paleo-subsurface river systems, extending about 93 km in cumulative length, which developed during the deposition of the Lianglitage Formation (Upper Ordovician) in the study area. This investigation concentrates explicitly on the architectural characteristics and evolutionary processes of the subsurface river system adjacent to the F_I7 fault zone (Figure 2), as it represents a particularly significant and well-preserved segment of the overall drainage network.

At least three stages of karstification (i.e., O_2y-O_3t, O_3l-O3s, O_3s-S) have been documented (Ma and Duan, 2023), herein the paleo-karst topography maps of three stages were presented (Figure 2). In general, a north-high and south-low feature, with a certain degree of inheritance, characterize the paleo topographies of the three periods. Specifically, after the deposition period of the Yijiafang Formation (Figure 2A), the terrain has minor undulations, and the river systems are of smaller scale and poor continuity. Following the deposition period of the Lianglitage Formation (Figure 2B), the terrain exhibits significant undulations, forming a gentle slope with a steep gradient, which results in the development of large-scale surface river systems extending from north to south. After the deposition period of the Sangtamu Formation (Figure 2C) and before the deposition of the Silurian strata, the topography essentially inherits the early structural pattern. Still, the scale of the river systems is noticeably reduced.

This subsurface river traverses the northern subsurface mountainous region, extends into the southern inter-bed karst zone, and merges with the surface river in this area, with an overall length of approximately 6.5 km, primarily distributed along the F_I7 strike-slip fault (Figure 2B). From north to south, based on the karst hydrological system classification, the paleo-subsurface river system can be categorized into a recharge zone, a runoff zone, and a discharge zone.

The seismic and geological characteristics of the paleo-subsurface rivers exhibit variations across these three zones. In the recharge zone, the paleo-subsurface river predominantly aligns with the fault direction, trending northeast, but interlaces with northwest-oriented channels, creating a network of river confluences, with the river repeatedly crossing the fault for development. In the runoff zone, the paleo-subsurface river develops along the left wall of the fault, trending northeast, primarily as a single channel. In the discharge zone, the paleo-subsurface river diagonally cuts through the fault and extends southward, shifting its orientation from northeast to northwest.

Both the RMS (Root Mean Square) attribute (Figure 3A) and tensor attribute (Figure 3B) exhibiting a notable degree of similarity between them can reflect the characteristics of the subsurface river in the Tarim Basin (Figure 3). Based on the observation from attribute maps, this paleo-subsurface river has not formed a complete and contiguous strong attribute reflection (Figure 3). The paleo-subsurface river is characterized by the presence of local high-energy bright spots that are weakly interconnected. The amplitude response characteristics of paleo-subsurface rivers differ slightly from north to south. In the northern region, these spots link to form a linear feature with intense attribute energy. In contrast, in the southern region, the structure predominantly manifests as point-like features with decreased attribute energy.

From north to south, the characteristics of the paleo-subsurface rivers exhibit significant variations across the distinct karstic

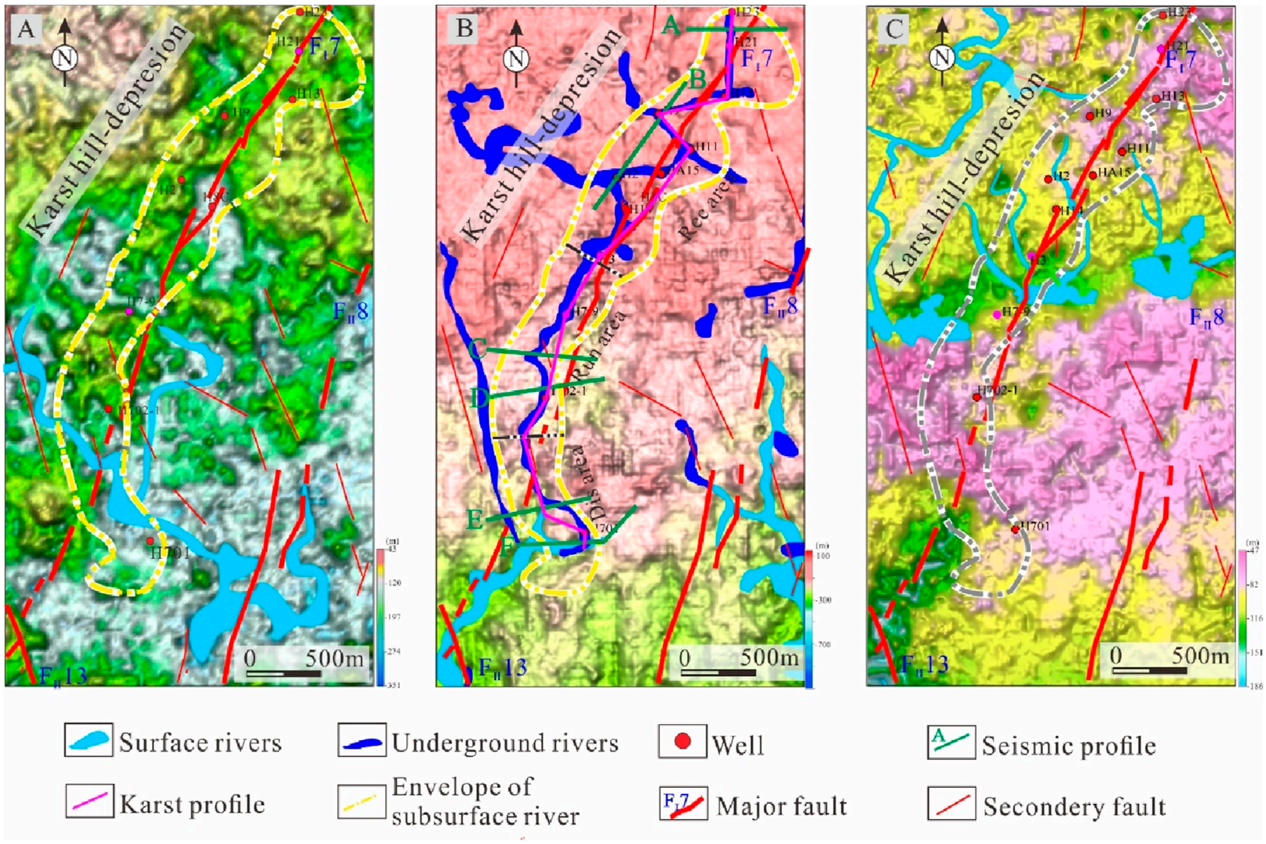

FIGURE 2
The surface rives and paleo-subsurface rivers overlapping on the paleo-karst topography maps after the periods of Yijianfang **(A)**, Lianglitage **(B)**, and Sangtamu **(C)** formations in the Halahatang area (see location in Figure 1A).

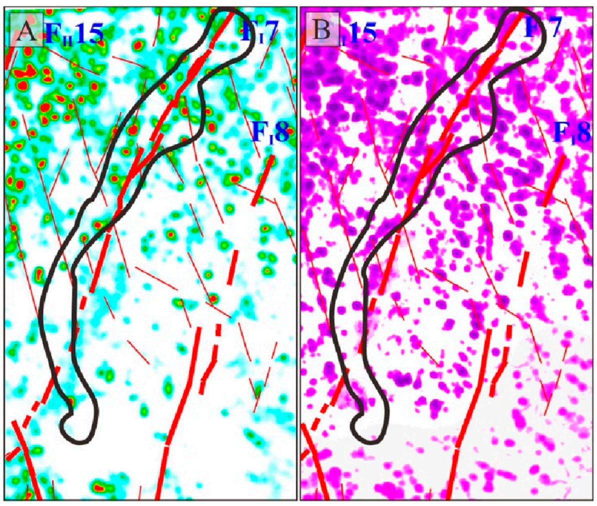

FIGURE 3
The RMS attribute **(A)** and tensor attribute **(B)** spacing 0–100 m (see location in Figure 1A; the red lines with different thickness indicate strike-slip faults, and the grey solid line indicates the extent of the subsurface river).

zones on the seismic profiles (Figure 4). In the recharge zone (Figures 4A, B), the paleo-subsurface rivers predominantly display strong amplitude reflections with a defined width, indicating a relatively shallow development, mainly occurring within the first member of Yingshan Formation, and developing downward from the weathered crust at the base of the Tumuxiuke Formation, with a progressively diminishing scale. In the runoff zone (Figures 4C, D), the scale of the paleo-subsurface rivers contracts, extending more deeply, characterized by strong amplitude reflections at the upper part and weak amplitude reflections at the lower part, indicating that the paleo-subsurface river no longer develops immediately adjacent to the weathered crust at the base of the Tumuxiuke Formation. In the discharge zone (Figures 4E, F), the paleo-subsurface rivers are positioned at an even greater depth, manifesting as intermittent and disorganized weak reflections, with occasional occurrences of more extensive strong amplitude reflections in localized areas.

4.2 Fracture-cavity characteristics of wells

Six wells along the subsurface river were chosen to illustrate the differential fracture-cavity characteristics in the recharge zone,

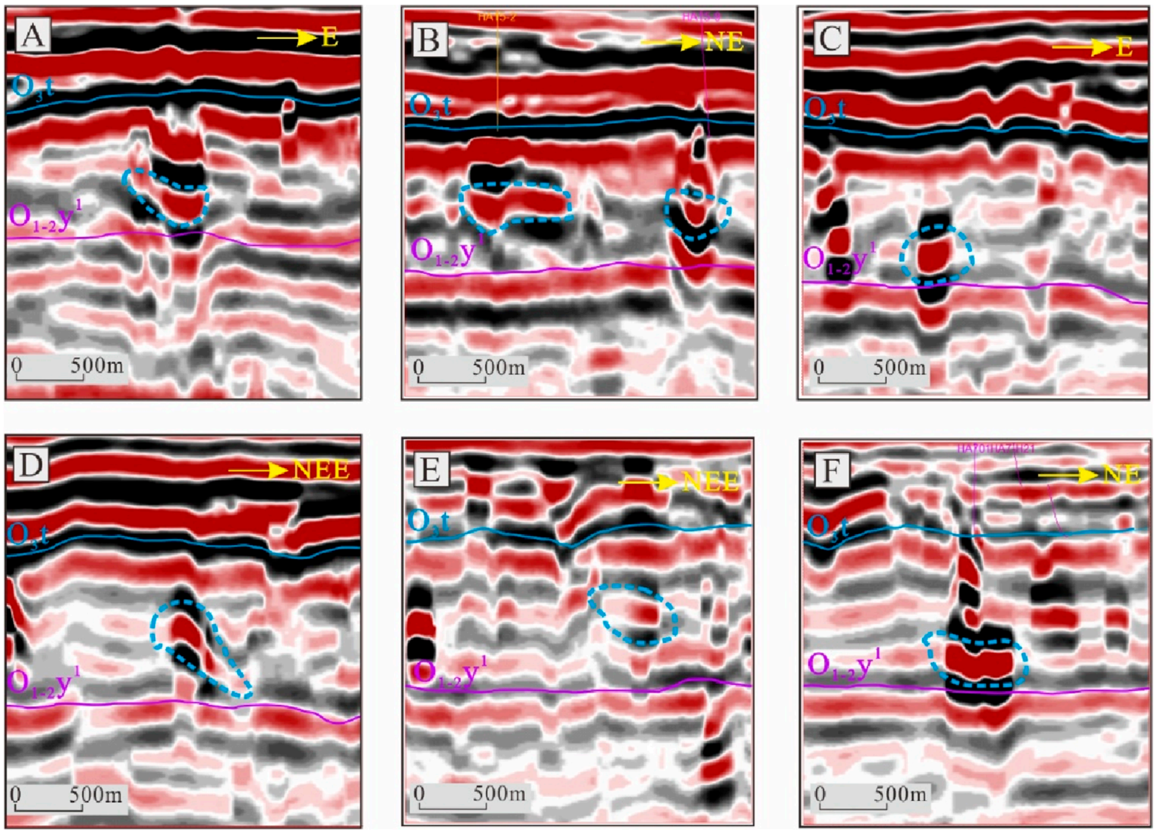

FIGURE 4
The characteristics of paleo-subsurface rivers in the recharge zone, runoff zone, and discharge zone on seismic profiles [see location in Figure 2; **(A, B)** - recharge zone; **(C, D)** - runoff zone; **(E, F)** - discharge zone]. The area within the blue dashed lines represents the boundary of the subsurface river's cross-section. $O_{1\text{-}2}y^1$ refers to the first member of the Yingshan Formation.

runoff zone, and discharge zone (Figure 5). All the fracture-cavity reservoirs were interpreted by the logging data, such as porosity curve and deep, sallow resistivity curves and so on. Three wells, H21, H9, and H4, displayed the fracture-cavity characteristics in the recharge zone. From 6,570 m to 6,620 m, fractures and cavities generally were nonuniformly distributed along the well. There is an empty area at the bottom of the well with a depth of 1.8 m, indicating a cave below. Identifying an empty with a thickness of 13.31 m at the bottom of well H9 suggests the presence of a fracture-cavity system of considerable magnitude, or it could be a segment of a subsurface river. Conversely, the absence of an empty interval in well H14 suggests that a paleo-subsurface river system may develop at depth. Upon integration with the seismic profile data, it is inferred that well H14 may not host a fracture-cavity system of significant scale. This assessment is crucial for understanding the geological and hydrogeological conditions of the area, which can guide further exploration and development strategies.

In the runoff zone, well H3 exhibits an empty at its base. Yet, the magnitude of this gap is minor compared to that observed in the recharge zone, implying the potential presence of a small-scale fracture-cavity system at the well bottom. Conversely, well H702-1 does not experience any empty across its entire section and only develops multiple class II and III reservoirs at greater depths. This suggests there may be localized fracture-cavity systems at certain intervals, but the reservoir quality is generally moderate.

In the discharge zone, well H701 exhibits an empty 1.78 m at the bottom, indicating the potential encounter with a scaled fracture-cavity reservoir. Combined with the seismic profile (Figure 4F), it will likely be a subsurface river.

Overall, the six wells along this paleo-subsurface river demonstrate that the development of the paleo-subsurface river channel is characterised by segmentation. There are also distinct differences across different areas (Figure 5). The subsurface mountain area exhibits overall favourable reservoir characteristics, signifying the development of a reservoir of a certain scale, and the substantial empty implies a larger scale of subsurface rivers. However, there are also areas of poor local reservoir quality, highlighting the segment of the subsurface rivers. The runoff and discharge zones are typically associated with less favourable reservoir types that develop near paleo-subsurface river systems. Additionally, in areas lacking distinct subsurface river development, reservoirs of inferior quality may also form under specific geological conditions.

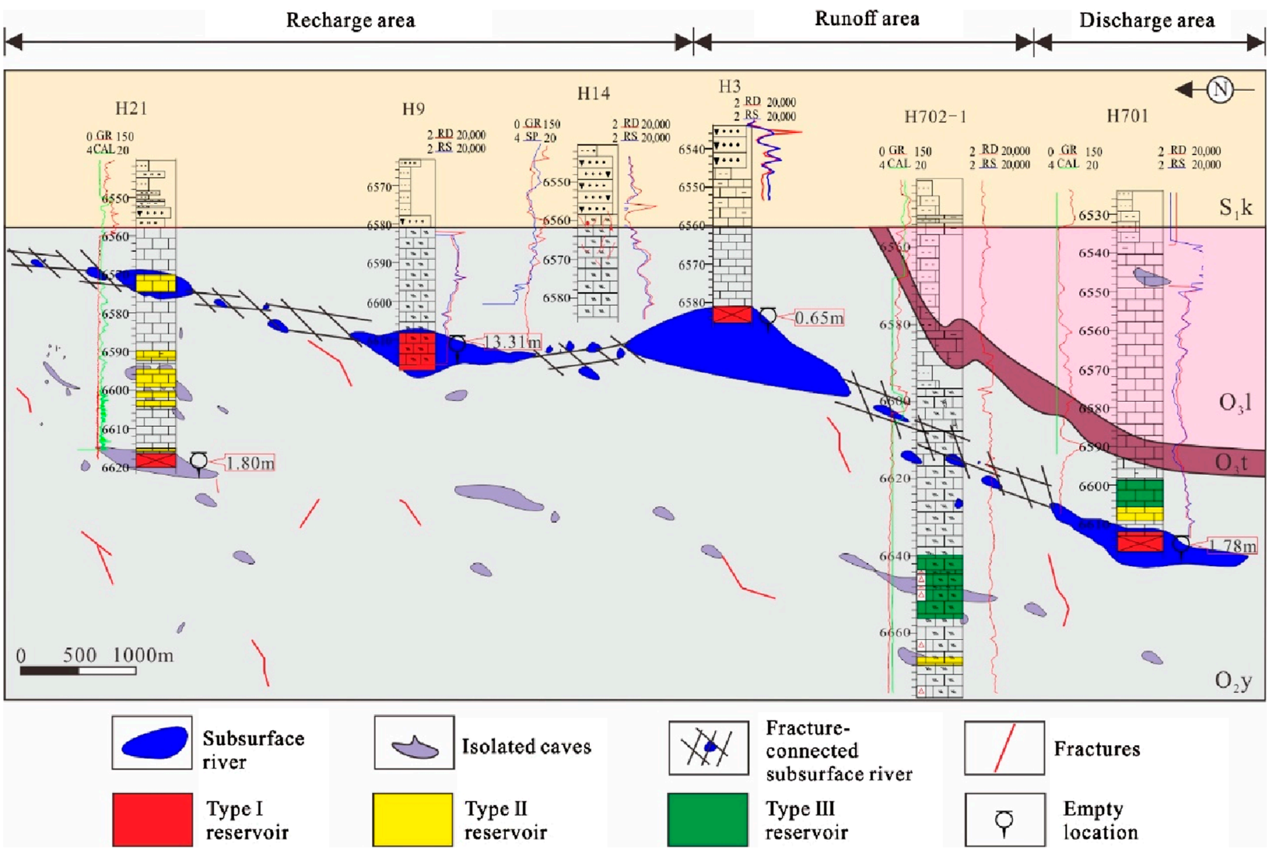

FIGURE 5
The characteristics of karst fracture/vug/cave in paleo-subsurface rivers (profile location is shown in Figure 2).

4.3 Reservoir characteristics of wells

4.3.1 Reservoir characteristics from core and thin section observation

The primary porosity of carbonate rocks in the Halahatang Oilfield is extremely low (porosity <2.5%; Du et al., 2010; Zhang et al., 2021), and observations from core thin sections show that secondary dissolution pores and micro-fractures are relatively well-developed. Based on the space and efficiency of the reservoir (Zhao et al., 2023), the Ordovician carbonate reservoirs are composed of four types, i.e., cavities, cavity-pores, pores-fractures, and fractures (Figure 6). Interpretations from drilling and well logging data reveal that the primary storage spaces of the carbonate rocks in the Halahatang Oilfield are dissolution cavities, solution-enlarged holes, and dissolution fractures (including tectonic fractures). Drilling and well-logging data indicate that cavity-like reservoirs are often identified by incidents of drilling interruptions and the occurrence of fluid loss (Figure 5). The extent of these drilling interruptions and the volume of fluid lost can provide a general indication of the scale and interconnectivity of these cavernous formations. This data is also an important indicator for reflecting the position of the paleo-subsurface river in the appropriate position.

Notably, these cavities and fractures are essentially filled and cemented (Figure 6). On the core, local fractures exhibit partially filled structures. In contrast, some cavities are filled with filling materials, including mud, breccia, calcite, and pyrite (Figures 6A–C). These fillings demonstrate that dissolution processes control the study area and prove that collapse-filling behaviours occurred concurrently with dissolution, blocking most of the pores and cavities. The different styles of filling materials also indicate multiple karst environments, and the abundance of mud and breccia filling suggests that the collapse-filling is somewhat contemporaneous with karst development. Thin section observations have found that some cavities and micro-fractures retain unfilled parts (Figures 6D–F), indicating that karst processes have a constructive impact on the reservoir.

4.3.2 Reservoir characteristics along the subsurface river

The tensor attribute serves to represent the architectural and distribution characteristics of reservoirs, including the subsurface river in karst-related systems. Profiles of tensor attributes along the strike of the subsurface river can effectively illustrate the structural features and the variations present in various karstic regions, particularly between the northern and southern areas (Figure 7). The reservoir units are predominantly located within the stratigraphic interval that spans the Yijianfang Formation up to the first member of the Yingshan Formation. There are also indications of potential extensions both below the first

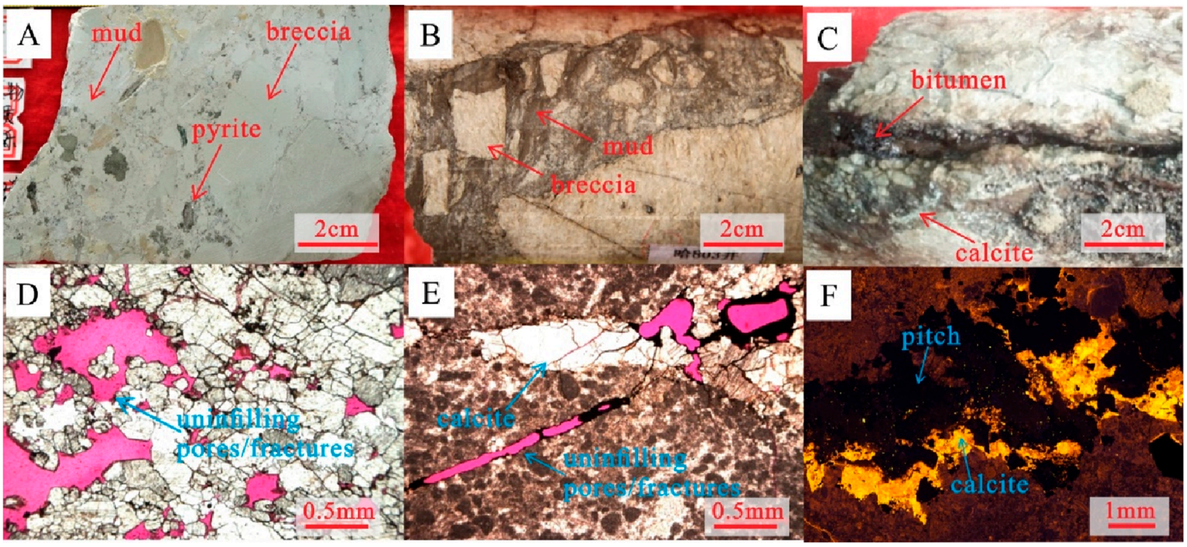

FIGURE 6
The typical characteristics of core and thin sections. **(A)** well J103, Yijianfang Formation, 7,226.32 m, a cave infilled by breccia, pyrite, mud-cement; **(B)** well H803, Yijianfang Formation, 6,615.61 m, a wide fracture infilled by mud, breccia; **(C)**, well H15, Yijiangfang Formation, 6,585.37 m, a half-infilled fracture is filled with mud, bitumen, and calcite; **(D)** well H803, Yijianfang Formation, calcite dissolution vugs, intercrystalline calcite pores, intra-bioclast pores, and occasional intergranular pores; **(E)** well H33, Yijianfang Formation, 6,618.6 m, dissolution fracture is filled or partially filled with calcite cement; **(F)** well X101, Yijianfang Formation, 6,811.0 m, dissolution fracture is filled with calcite and pitch).

member of the Yingshan Formation and upward into the Lianglitage Formation.

A pronounced segmentation pattern is evident in the fracture-cavity volumes along a south-to-north gradient. The northern region exhibits a greater density of fracture-cavity volumes, characterized by reduced spacing and shallower depths, typically within 150 m beneath the Yijianfang Formation. In contrast, the fracture-cavity volumes in the southern region are more widely spaced, characterized by lower development density and deeper extensions. Meanwhile, the fracture-cavity volumes in the northern region demonstrate a broader lateral extension along the course of the subsurface river. In the south, however, these volumes are sparsely developed, with limited extensions.

Statistical analysis indicates that variations in the width of fracture-cavity volumes, the distance from these volumes to the base of the Tumuxiuke Formation, and the cumulative production data show notable similarities. This suggests a positive correlation between the scale of fracture-cavity volumes and cumulative production. Generally, the width of the fracture-cavity volumes diminishes from the recharge zone through the runoff zone to the discharge zone, reflecting changes in the scale of the subsurface rivers and their associated fracture-cavity volumes. Some local increases in width may occur due to the influence of faults or other geological factors.

The height of the fracture-cavity volumes typically exhibits an initial increase followed by a decrease. This pattern correlates with the development of surface karst fracture-cavity volumes in the recharge zone, which results from prolonged erosion, as well as the formation of karstic channels in the runoff zone. In the discharge zone, a reduction in the scale of fracture-cavity volumes is observed, likely due to weakened hydrodynamic conditions. Notably, the fracture-cavity volume of Well H701 displays significant vertical extension with limited lateral spread, resembling the dissolution characteristics associated with strike-slip faults.

4.4 Geochemical characteristics of wells

Stable isotope analysis was conducted on 33 samples from the Yijianfang Formation. The $\delta^{13}C$ values of the selected samples exhibited significant variability, ranging from −3.75‰ to 1.5‰, while the $\delta^{18}O$ values spanned from −15.71‰ to −5.35‰ (see Figure 8 for details). The $\delta^{13}C$ and $\delta^{18}O$ values in different fillings exhibit distinct patterns, indicative of different filled stages. Within this stable isotopic variability three groupings and two outlier are distinguished that relate to the component and their isotope signatures (Figure 8). The groups are categorized as follows: (1) a diverse array of components, including calcite, mud, and siliceous clumps, which make up the largest group consisting of 18 samples with $\delta^{13}C$ values ranging from −2.45‰ to −0.02‰ and $\delta^{18}O$ values from 13.35‰ to −6.57‰. These values indicate an atmospheric freshwater karst environment within the exposed strata of the Yijianfang Formation. (2) A set of seven samples comprising mud and calcite, displaying low positive $\delta^{13}C$ values between 0.02‰ and 0.86‰, and low negative $\delta^{18}O$ values from −8.72‰ to −6.06‰, confirm a shallow buried environment associated with the Lianglitage stage. (3) Two samples of calcite exhibit highly positive $\delta^{13}C$ values ranging from 1.05‰ to 1.5‰ and low negative $\delta^{18}O$ values between

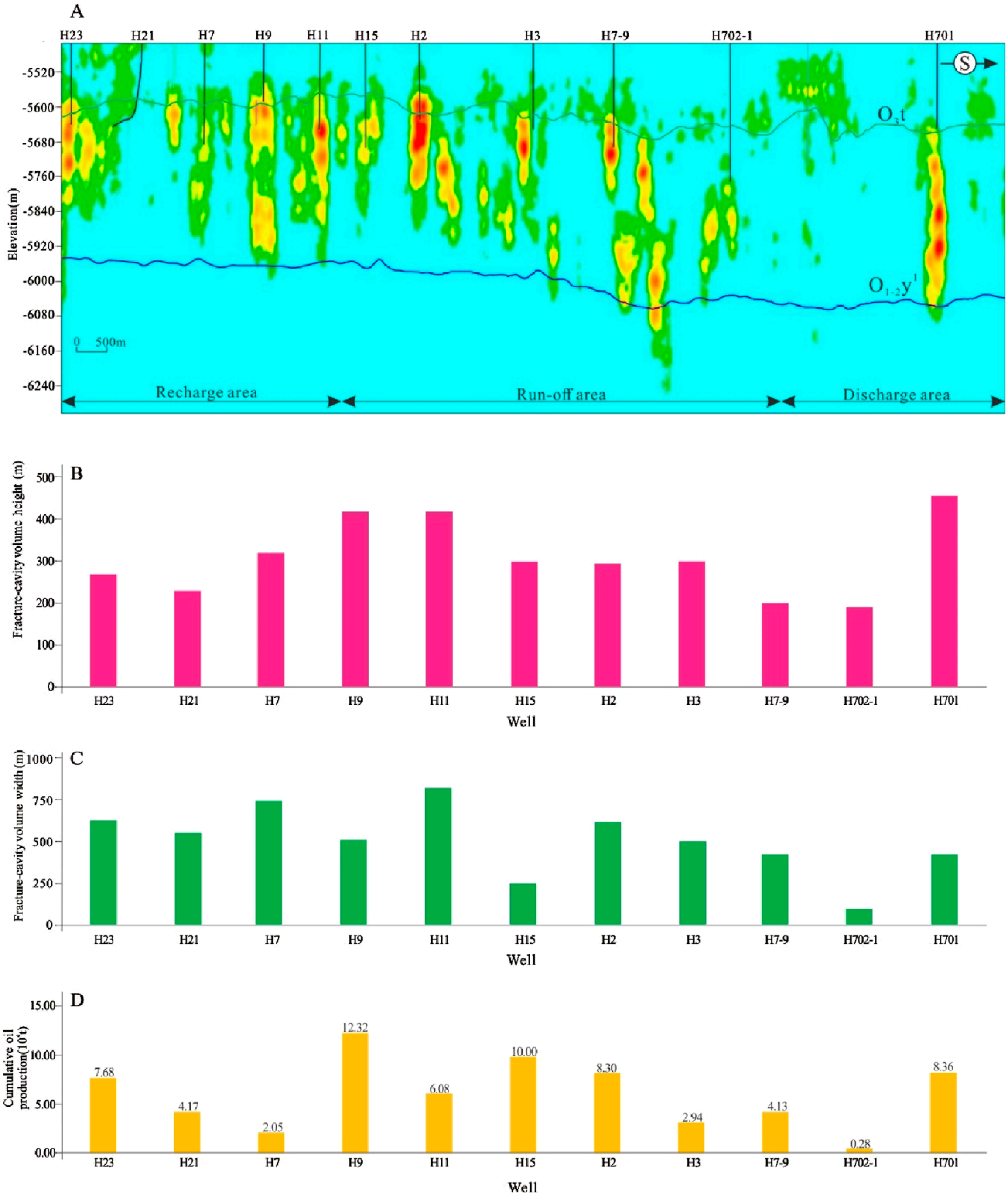

FIGURE 7
Tensor profile along the paleo-subsurface river **(A)** and statistical histograms of fracture-cavity volume height **(B)**, fracture-cavity volume width **(C)**, and cumulative production **(D)** of different wells along the paleo-subsurface river.

−7.17‰ and −5.35‰, indicating a deep buried environment from the Pre-Silurian period. (4) Another two samples of calcite show highly positive $\delta^{13}C$ values between −3.79‰ and −3.25‰, along with low negative $\delta^{18}O$ values from −15.17‰ to −13.08‰, suggesting local hydrothermal activity. (5) Finally, four samples of calcite present higher positive $\delta^{18}O$ values from −15.71‰ to −14.61‰ and low positive $\delta^{13}C$ values between −0.4‰ and 0.06‰, indicative of hydrothermal activity.

5 Discussion

5.1 Architecture of low-mature partially through-going paleo-subsurface rivers

Subsurface rivers typically have distinct recharge, runoff, and discharge systems, with larger systems forming interconnected subterranean hydrological networks that include a primary channel

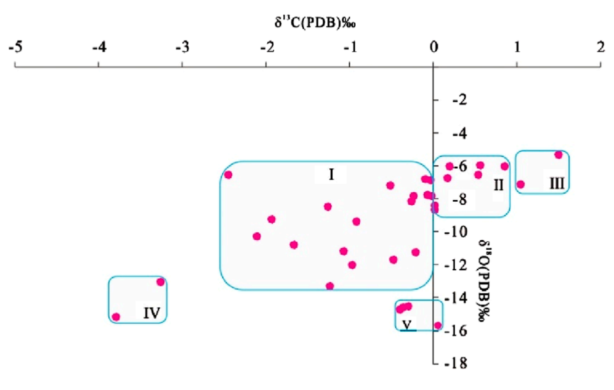

FIGURE 8
Stable isotope plot ($\delta^{13}C$ *versus* $\delta^{18}O$) of carbonate fracture-cavity fillings within the Yijianfang Formation in the Halahatang area.

and its branches (Zhang et al., 2021; Chen et al., 2022; Dong et al., 2024). The evolution of these rivers is influenced by topography, lithology, fractures, and exposure duration, often resulting in irregular patterns (Zhang, 2018; Zhang et al., 2021; Dong et al., 2024). Despite this, the fundamental structure of a subsurface river system is composed of a primary channel and its branches, with the primary channel extending over a greater distance and being more substantial in scale (Dong et al., 2024). In contrast, branches exhibit a more complex morphology and are shorter, shallower, and smaller in scale (Yuan, 1993). Some narrow subsurface rivers manifest linear, point-like strong amplitudes on the seismic profiles (Baaske et al., 2007; Burberry et al., 2016). In the Tahe Oilfield of the Tarim Basin, subsurface rivers often appear as a network of waterways with multiple branches converging into a main channel, which can be found through seismic profiles and planar attributes, revealing their distribution characteristics (Xu et al., 2022; Chen et al., 2023; Dong et al., 2024).

Based on seismic structural features and well logs, the paleo-subsurface rivers in the Halahatang area generally display a discontinuous, fragmented linear structure with varying degrees of connectivity across different karst regions (Figure 9; Li et al., 2021; Qiao, 2020). In the recharge zone, subsurface rivers are relatively more prolonged, wider laterally, and have a shallower longitudinal extension, interacting strongly with surface river systems or local systems. This area also develops branch channels that link to the major fault, characterised by point-like strong amplitude reflections (Figure 4), yet they do not fully connect with the major fault. In the runoff zone, the subsurface rivers shorten in length but maintain a certain extension, deepening longitudinally, likely due to the significant hydraulic gradient in this area. However, they become relatively narrower laterally, possibly due to the weaker hydrodynamic action under the short-term exposure of the slope. In the discharge zone, the extension of the subsurface rivers is sharply reduced, with the local development of strong dissolution segments that have very poor connectivity, potentially related to the prevalent conjugate strike-slip faults in the Halahatang area (Wei, 2018; Ning et al., 2021; Qiao, 2020; Shang et al., 2020). These dissolution segments constitute the principal framework of the karst paleo-subsurface river system, which is characterised by a scarcity of tributary channels within the region (Ren and Liu, 1983; Zhang et al., 2020b; Zhang et al., 2022b; Yang et al., 2023). There is a pronounced diminution in their potential to extend southward, where they frequently converge with and dissipate into the superficial river networks across an extensive inclined terrain.

The northeastern uplift of the Halahatang area, the Tahe Oilfield, has confirmed the presence of a large-scale subsurface river system characterised by multiple phases of infilling (Ding et al., 2020; Jiang and Li, 2021; Chen et al., 2023; Dong et al., 2023; Dong et al., 2024). This includes typical features of dissolution collapse and argillaceous sediment infilling, with the infilling characteristics of the subsurface rivers exhibiting clear patterns of evolution and migration (Lei et al., 2014; Jin et al., 2015; Li et al., 2023; Dong et al., 2024). However, in the Halahatang area, typical multi-phase infilling is seldom observed (Zhang, 2018). Some dissolution cavities contain extremely fine-grained argillaceous sediments and are cemented by calcite (Figure 6), indicative of a subdued hydrodynamic environment and a relatively constrained subsurface river system. Although wells encountering these subsurface rivers may experience gas release and leakage, this also implies the limitations of the karst channel system (Dan et al., 2016; Ding et al., 2020). Once the paleo subsurface river system is established, the internal infilling and the calcite cementation of the cave's roof fractures gradually seal the channels (Jin et al., 2015; Jiang and Li, 2021; Lei et al., 2014). For the Halahatang area, these geological conditions are highly favourable for the formation of a partially connected subsurface river system and are also conducive to preserving the development of high-quality fracture-cavity volumes on a certain scale (Ning and Hu, 2020; Chen et al., 2023; Yang et al., 2020).

5.2 Evolutionary process of low-mature paleo-undergrounder rivers under multi-stage tectonostratigraphic evolution

The Halahatang area has experienced multiple phases of karst superimposed transformation, including the period of the Yijianfang Formation, the period of the Lianglitage Formation, the period of pre-Silurian, and the deep-burial period (Figure 8; Peng et al., 2009; Zhang, 2018; Chen et al., 2023). The periods of the Yijianfang and the Lianglitage formations are critical times for the formation of karst fractures and cavities in carbonate rocks, especially the karst activity during the period of Lianglitage Formation, which is the key period for the formation of karst fracture-cavity reservoirs in the Halahatang Oilfield (Zhu et al., 2011; Du et al., 2010; Zhang et al., 2018; Zhang, 2018). Combined with the results of paleo-topography reconstruction and regional tectonic movements, it is believed that the Halahatang area is controlled by different tectonic movements in multiple phases, leading to differences in karst activity, which in turn affects the formation and evolution of paleo-subsurface rivers (Peng et al., 2009; Du et al., 2010). Based on the dissection results of the subsurface river in the Halahatang area, the low-mature, partially through-going subsurface river system has been systematically reconstructed into four distinct stages: the initial formation stage, the expansion and growth stage, the differential connectivity stage, and the burial-compaction with localised compaction stage. This multi-stage model provides a robust framework for understanding

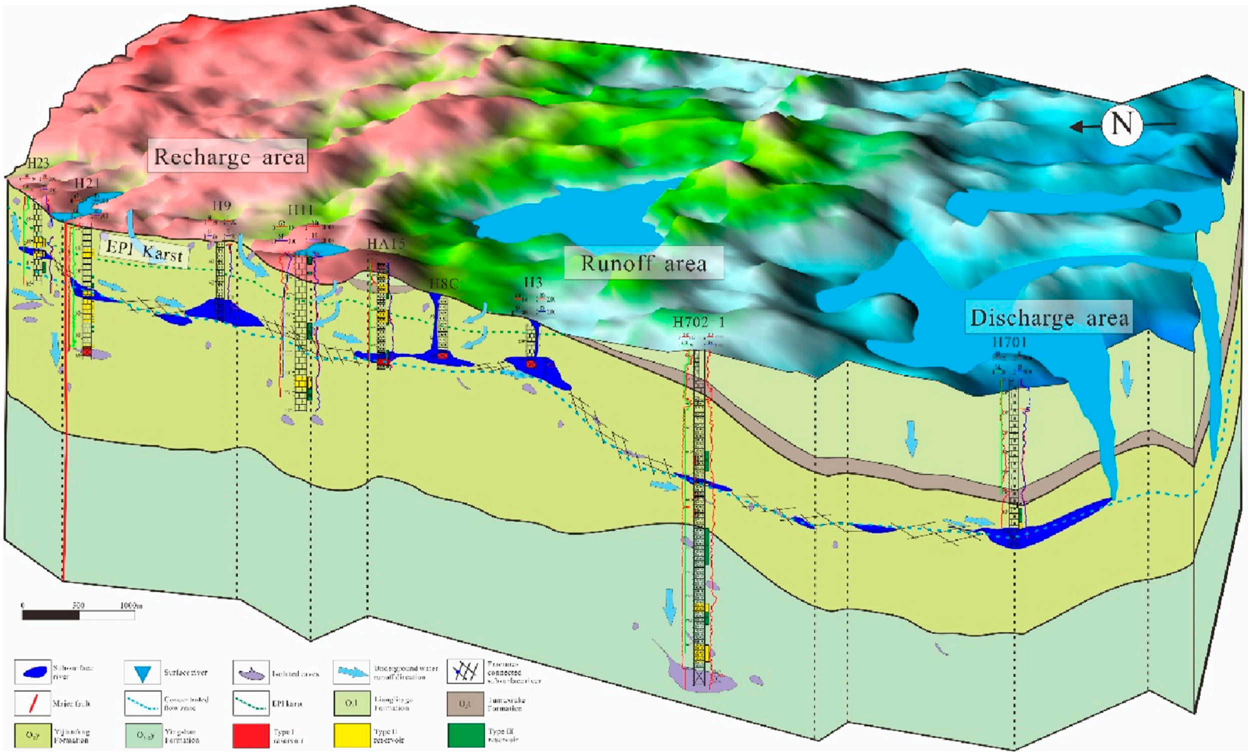

FIGURE 9
The 3D geological model of the typical subsurface river channel in the Halahatang area.

the subsurface river system's developmental dynamics and structural modifications over time.

1) The initial stage is characterised by isolated subsurface rivers (Figure 10A). At the end period of the Yijianfang Formation, the paleo-karst topography reconstruction map of this period shows that the area had features of micro-landform development, with short water systems and a low hydraulic gradient (<0.2%). This is a short hiatus (1.5~2 Ma) with mid-negative values of stable isotope (Shi et al., 2015; Chen, 1994; Figure 7), and only 2–4 conodont spina bands were missing (Yu, 2005; Zhang et al., 2005; Bao et al., 2007). Atmospheric precipitation and surface runoff mainly infiltrate the dissolution zone vertically through fault damage zones or their influence zones, and near the groundwater level, lateral flow along the fault-broken belts predominates, with no obvious concentrated groundwater flow (Chen, 1994; Loucks, 1999; Loucks and Mescher, 2002; Zhang et al., 2005; Onac, 2014; Shi et al., 2015). The groundwater flow is slow, the depth of karst action is shallow, and karst fractures and caves only develop within a 0–30 m range below the top surface of the Yijianfang Formation (Lu et al., 2018; Ning et al., 2021). During this period, karstification mainly occurs along faults or in some local easy-dissolution areas, possibly related to lithology or sedimentary facies. The ~460 Ma dating ages from calcite cement samples (Wu et al., 2012c; Yang et al., 2022; Ma et al., 2024) and a significant proportion of the samples (Figure 8) also suggest this karst period. The paleo-subsurface river was widely distributed as isolated point-like or short-line types in various parts of the study area, controlled by local strong fault activity or local highs in lithology or sedimentary facies (Figure 2A). This forms the foundation for the forthcoming subsurface river. Consequently, this phase represents the preliminary stage of the subsurface river.
2) The expansion growth stage occurs after the period of the Lianglitage Formation in the Halahatang area (Figure 10B). The study area underwent shallow buried karst, which was affected by CH_4 and less vaporization, with stable isotope showing slightly positive values of $\delta^{13}C$ and slightly negative values of $\delta^{18}O$ (Liu et al., 2014; Dong et al., 2023; Dong et al., 2024). Under the control of tectonic activity, the overall topography of the Halahatang area is higher in the north and lower in the south, with a platform margin formed in the southern slope area, and intense erosion and karstification in the north (Zhao et al., 2008; Zhang, 2018; Ning et al., 2021). Karst activity in the south is weaker under a micro-geomorphological combination during the period of the Lianglitage Formation, with water systems generally flowing from north to south or south with an easterly bias (Liu et al., 2014; Wei, 2018). During this period, the hydraulic gradient is relatively large, and an extended surface river system develops on the top of the Lianglitage Formation (Zhang, 2018; Ning et al., 2021). The C/O isotope is similar between mud infillings of fractures in the Yijiangfang Formation (0.02‰ $\delta^{13}C$, −8.72‰ $\delta^{18}O$) and mud filling in the caves in the Lilitage

Formation (0.02‰δ^{13}C, −8.28‰δ^{18}O) (Figure 8), indicating the connection between subsurface rivers in Yijianfang Formation and rivers in Lianglitage Formation under strong hydrodynamic force (Zhang, 2018; Ning et al., 2021). Based on the early karst period of the Yingshan Formation and Yijianfang Formation, the underground flow may form a partially connected paleo-subsurface river. This water flow is composed of early dissolution-enlarged and extended dissolution cavities linked through fractures or the original pore network of the rock, forming a connected system of pores and fractures. This stage is so essential that formed the subsurface river network during this period.

3) The differential connectivity stage precedes the Silurian deposition in the Halahatang area (Figure 10C), which undergoes an episode of uplift, exposure, and erosion (Peng et al., 2009; Li et al., 2015; Ma and Duan, 2023). This period is marked by an extended duration of exposure, with a topographical gradient that slopes from higher elevations in the north to lower ones in the south, accompanied by a substantial hydraulic gradient (Liu et al., 2014; Li et al., 2015; Zhang, 2018). A surface river system, predominantly oriented in the northwest direction, develops at the top of the Ordovician strata. Under these conditions, the early subsurface rivers within the Yingshan to Yijianfang formations continue to expand and evolve. However, they are constrained by factors such as exposure duration, hydrodynamic conditions, and climate, preventing the subsurface rivers from fully penetrating to form a completely interconnected network of fracture-cavity volumes (Palmer, 1991; Palmer, 2007; Loucks, 1999; Klimchouk, 2009a; Klimchouk, 2009b; Mcmechan et al., 2002; Hollis and Sharp, 2011). The stages of erosion and infilling within the subsurface rivers are not clearly defined, and a significant number of cavities persist (Liu et al., 2014; Dong et al., 2023; Dong et al., 2024). Highly positive values of δ^{13}C and low negative values of δ^{18}O (Figure 8) indicate the substantiated deep burial karst environment (Liu et al., 2014; Shi et al., 2015; Dong et al., 2023; Dong et al., 2024). Under the superposition of topography and faults in peak cluster depressions, karst fractures and cavities are further developed, and some isolated fractures and cavities that are not connected are gradually connected (Chen et al., 2024; Ma et al., 2024). At the location of the discharge area, due to the obstruction of Silurian clastic rocks in the southward runoff of surface water systems, some surface water systems form karst lakes at this location, and some surface water systems flow southward underground along the fault zone. The above geological conditions have led to poor drainage of the subsurface river, resulting in partial filling (Dong et al., 2024). The forward and reverse filling of the subsurface river occur simultaneously, and this stage is the mature stage of subsurface river development.

4) The burial-compaction and local compaction stage (Figure 10D). Throughout the subsequent stages of shallow to deep burial, despite the possibility of significant erosion occurring before the deposition of Carboniferous strata in the Northern Tarim Basin, this did not result in the creation of an erosional surface in the Halahatang area. Consequently, this limited the continued influence of karst processes on the early paleo-subsurface rivers. Despite the potential for local hydrothermal karst activity due to the development of the Permian Large Igneous Province (Li et al., 2015; Ma and Duan, 2023), the study area is predominantly influenced by the thickening of the overlying rock strata, leading to a gradual compaction. The early fracture-cavity network segments, characterised by the interplay of lithologic porosities and fractures, may undergo cementation or compaction, resulting in the spatial formation of isolated or weakly connected short-line subsurface rivers.

5.3 Influence of low-mature partially through-going paleo-undergrounder rivers on reservoir distribution and hydrocarbon accumulation

Potential reservoirs within a subsurface river system are identified as the primary channel of the subsurface river, its branches, and the fracture zones above the subsurface river, often referred to as "cave roof fractures" (Lei et al., 2014). The main channel acts as the principal pathway for water flow within the entire subsurface river system (Li, 2012). Integrating the discussions and analyses presented, it is conceivable that the upper fracture zone of the subsurface river may be partially cemented, which could be observed in thin sections, cores (Figure 6), and logging data (Figure 5). These segments, which are not fully connected and are locally preserved, represent excellent fracture-cavity reservoir volumes. However, influenced by distinct tectonic movements and the associated karst processes, the Halahatang area has given rise to various karst zones, including the buried-hill karst zone, inter-bedded karst zone, and fault-controlled karst zone (Zhang, 2018). The structural variations of paleo-subsurface rivers within these karst zones further impact the development of subsurface river reservoirs, as well as the types and evolutionary formation of hydrocarbon reservoirs (Machel et al., 2012).

In the buried hill area, karstification of varying intensities occurred during three critical periods following the deposition of the Yijianfang Formation, the Lianglitage Formation, and before the Silurian. Within the study area, the majority of the Yijianfang Formation has been significantly eroded. The paleo-subsurface rivers are interconnected with the surface weathering crust, resulting in the formation of blocky or locally stratified fracture-cavity reservoirs. Some of these reservoirs have been filled with Silurian argillaceous sediments. The oil and gas reservoir types resemble those found in the Tahe area, albeit on a smaller scale, and are frequently altered by the weathering crust (Lei et al., 2014; Jin et al., 2015; Jiang and Li, 2021). Consequently, the scale of oil reservoirs associated with paleo-subsurface rivers tends to be smaller. Exploration potential is better directed towards areas influenced by a combination of factors, including the weathered crust, ancient subsurface rivers, local highs, and zones of fault development (Yang et al., 2022; Chen et al., 2023). Furthermore, before Silurian deposition, the concealed mountain region experienced a degree of erosion, leading to the dissipation of oil and gas, particularly that of paleo-subsurface rivers, which were formed during the middle to late Caledonian (Dan et al., 2016; Zhang, 2018; Ding et al.,

10.3389/feart.2025.1484909

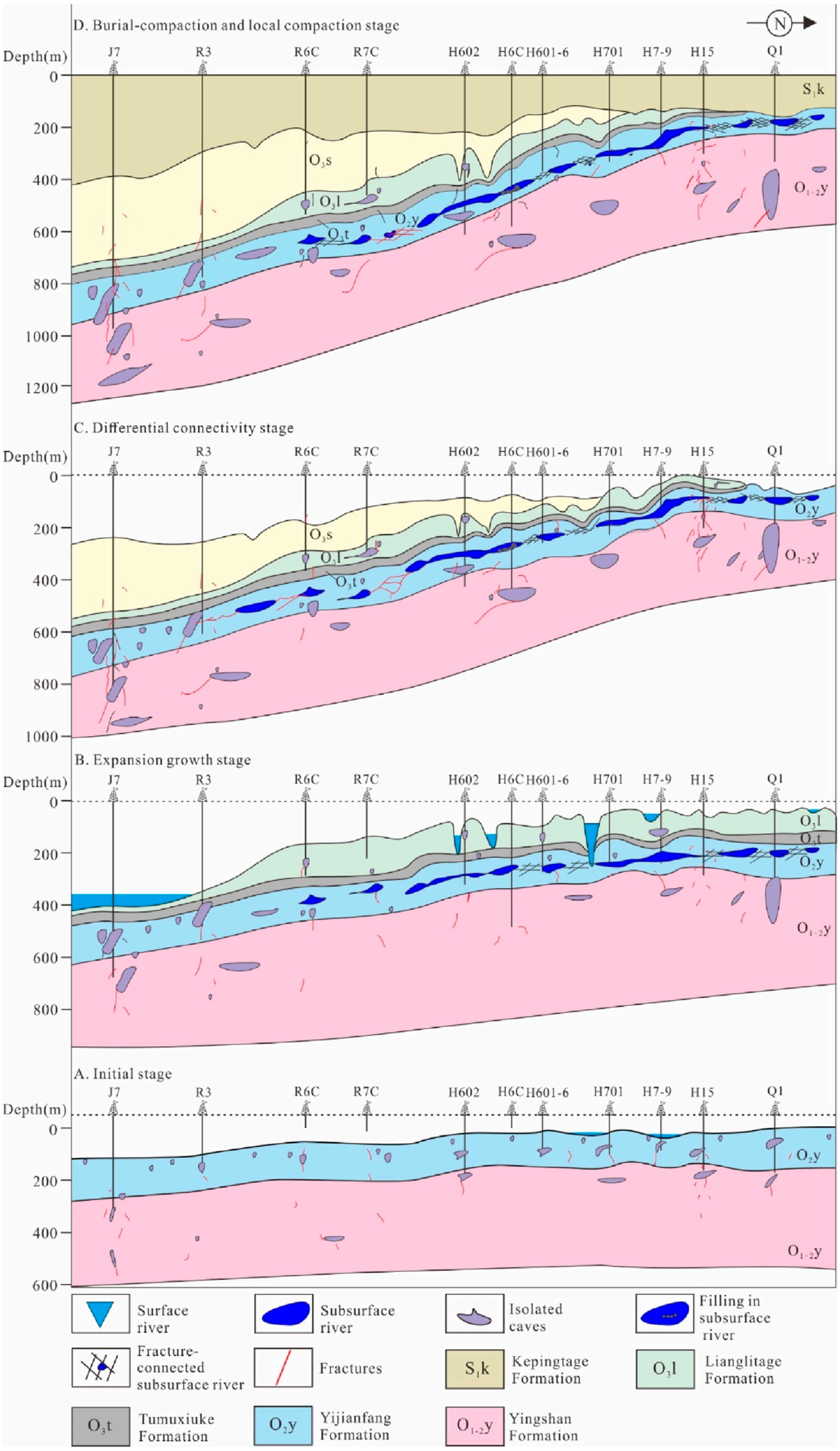

FIGURE 10
The formation and evolutionary process of the paleo-subsurface river in the Halahatang area. **(A)** Initial stage, **(B)** Expansion growth stage, **(C)** Differential connectivity stage, **(D)** Burial-compaction and local compaction stage.

2020). This is detrimental to the preservation of reservoirs. The region is often the recipient of oil and gas influx during the Hercynian or even later periods (Zhao et al., 2008; Lu et al., 2009; Liu et al., 2014; Yang et al., 2022).

In the interlayer karst area, three principal karstification periods have contributed to the formation of discontinuous paleo-subsurface river reservoirs of significant scale, which remain intact (Zhang, 2018). Following the interaction with strike-slip faults at various locations, it is prone to the development of fault-fracture zones and subsurface river reservoirs, as well as fault-connected subsurface river reservoirs within the sealed ancient underground rivers (Zheng et al., 2015; Yang et al., 2022). This karst zone is favourable for retaining oil and gas from the Caledonian period, allowing for the formation of early reservoirs that undergo subsequent adjustments and modifications under tectonic influences, along with Hercynian oil and gas injections in later periods (Zhu et al., 2011). The oil and gas reservoirs within the discontinuous channels in the Halahatang area are resistant to compaction and destruction, signifying a potential focal point for research across the entire slope region. Consequently, ongoing efforts in seismic delineation of paleo-underground rivers, development of segmented models for paleo-subsurface rivers that are not fully penetrated, and the clarification of boundaries are specific research areas for exploring the potential of this region. The fault-controlled zone, which generally lacks subsurface river development, is not subject to analysis in this context.

6 Conclusion

1) The paleo-subsurface river system in the Halahatang area is characterised by discontinuous, southward-dipping conduits that demonstrate progressively increasing discontinuity and decreasing scale along the hydrodynamic gradient from the recharge zone through the runoff zone to the discharge zone.
2) The formation and evolutionary development of paleo-subsurface river systems can be categorised into four distinct stages. The initial stage is characterised by the development of isolated, small-scale conduits with limited connectivity. This is followed by a prolonged period of intensive karstification, during which the initially isolated channels interact and coalesce, forming partially interconnected fracture-cavity networks. The third stage witnesses the establishment of a fracture-connected subsurface river system exhibiting variable scales through maintaining channel discontinuity. Finally, during subsequent deep burial diagenesis, the fracture-cavity connections within these discontinuous channels undergo cementation and compaction processes, resulting in the formation of discontinuous subsurface river systems.
3) The structure and evolution of the partially thorough-going subsurface rivers influence the distribution of reservoirs, which are characterised by isolated, discontinuous patterns with a reduction in scale towards the south. In the runoff zone, the reservoirs are the largest and most complex, and when coupled with faults, they can form subsurface river-related reservoirs, creating favourable areas for hydrocarbon accumulation.

Data availability statement

The original contributions presented in the study are included in the article/supplementary material, further inquiries can be directed to the corresponding author.

Author contributions

HD: Conceptualization, Data curation, Funding acquisition, Investigation, Methodology, Project administration, Writing–original draft, Writing–review and editing. BM: Conceptualization, Data curation, Investigation, Methodology, Writing–review and editing. XW: Resources, Writing–original draft. JL: Formal analysis, Writing–original draft. BL: Data curation, Writing–review and editing. QZ: Methodology, Writing–review and editing. MZ: Software, Writing–original draft. GM: Investigation, Writing–original draft.

Funding

The author(s) declare that financial support was received for the research, authorship, and/or publication of this article. This research was funded by Basic Research Funds of the Chinese Academy of Geological Sciences (JKYQN202367), Guangxi Key Research and Development Plan Project (AB23026062), Basic Research Funds of Chinese Academy of Geological Sciences (2022011).

Acknowledgments

We appreciate PetroChina Tarim Oilfield Company's data support.

Conflict of interest

Author XW was employed by PetroChina Tarim Oilfield Company.

The remaining authors declare that the research was conducted in the absence of any commercial or financial relationships that could be construed as a potential conflict of interest.

Publisher's note

All claims expressed in this article are solely those of the authors and do not necessarily represent those of their affiliated organizations, or those of the publisher, the editors and the reviewers. Any product that may be evaluated in this article, or claim that may be made by its manufacturer, is not guaranteed or endorsed by the publisher.

References

Arosi, H. A., and Wilson, M. E. J. (2015). Diagenesis and fracturing of a large-scale, syntectonic carbonate platform. *Sediment. Geol.* 326 (AUG.1), 109–134.

Audra, P., D'antoni-Nobecourt, J. C., and Bigot, J. Y. (2010). Hypogenic caves in France. Speleogenesis and morphology of the cave systems. *Bull. Soc. Geol. Fr.* 181, 327–335. doi:10.2113/gssgfbull.181.4.327

Baaske, U. P., Mutti, M., Baioni, F., Bertozzi, G., and Naini, M. A. (2007). "Using multi-attribute neural networks classification for seismic carbonate facies mapping: a workflow example from the mid-Cretaceous Persian Gulf deposits," in *Seismic geomorphology*. Editors R. J. Davies, H. W. Posamentier, L. J. Wood, and J. A. Cartwright eds (London: Geological Society), 277, 105–120.

Bao, Z. D., Qi, Y. C., Jin, Z. J., Zhang, X. L., Hu, G. C., Zhang, Q. H., et al. (2007). Karst development response to sea-level fluctuation: a case from the Tarim area in the early Paleozoic. *Acta Geol. Sin.* 81 (2), 205–211. doi:10.3321/j.issn:0001-5717.2007.02.009

Burberry, C. M., Jackson, C. A. L., and Chandler, S. R. (2016). Seismic reflection imaging of karst in the Persian Gulf: Implications for the characterization of carbonate reservoirs. *AAPG Bulletin* 100 (10), 1561–1584.

Chen, H. X., Kang, Z. H., and Kang, Z. J. (2022). Stratified structure and formation mechanism of paleokarst cave in carbonate reservoir of Tahe oilfield. *Geoscience* 36 (2), 695–709. doi:10.19657/j.geoscience.1000-8527.2022.193

Chen, L. X., Jia, C. Z., Jiang, Z. X., Su, Z., Yang, M. C., Yang, B., et al. (2023). Oil enrichment model and main controlling factors of carbonate reservoirs in Halahatang area, Tarim Basin. *Acta Pet. Sin.* 44 (6), 948–961. doi:10.7623/syxb202306005

Chen, L. X., Wang, S. L., Jiang, Z. X., Zhu, G. Y., Su, Z., and Hou, J. K. (2024). Fault characteristics, reservoir types and distribution prediction in a fault-controlled area in the Ordovician strata of the Thebe Block, Halahatang Oilfield. *Petroleum Sci. Bull.* 9 (3), 408–421. doi:10.3969/j.issn.2096-1693.2024.03.030

Chen, R. K. (1994). Application of stable oxygen and carbon isotope in the research of carbonate diagenetic environment. *Acta Sedimentol. Sin.* 12 (4), 11–21.

Culver, D. C., and Pipan, T. (2019). *Subterranean ecosystems*. Amsterdam: Elsevier.

Dan, Y., Zou, H., Liang, B., Zhang, Q. Y., Cao, J. W., Li, J. R., et al. (2016). Restoration of multistage paleogeomorphology during Caledonian Period and paleokarst cavernous reservoir prediction in Halahatang area, northern Tarim Basin. *Oil and Gas Geol.* 37 (3), 304–312. doi:10.11743/ogg20160302

Davies, G. R., and Smith, L. B. (2006). Structurally controlled hydrothermal dolomite reservoir facies: an overview. *AAPG Bull.* 90, (11), 1641–1690. doi:10.1306/05220605164

Ding, Z., Wang, R., Chen, F., Yang, J., Zhu, Z., Yang, Z., et al. (2020). Origin, hydrocarbon accumulation and oil-gas enrichment of fault-karst carbonate reservoirs: a case study of Ordovician carbonate reservoirs in South Tahe area of Halahatang oilfield, Tarim Basin. *Petroleum Explor. Dev.* 47 (2), 306–317. doi:10.1016/s1876-3804(20)60048-9

Dong, H. Q., Liang, J. P., Zhang, Q. Y., Li, J. R., Wan, J. W., Nie, G. Q., et al. (2024). The differential collapse–filling evolution process of the paleo-underground river in the Northern Uplift of the Tarim Basin. *Front. Earth Sci.* 12, 1395384. doi:10.3389/feart.2024.1395384

Dong, H. Q., Zhang, Q. Y., Liang, J. P., Liang, B., Li, J. R., Dan, Y., et al. (2023). Carbon and oxygen isotopic characteristics of karst fracture-cavity fillings and environmental significance: a case study of Ordovician Yingshan Formation in Tahe Oilfield. *Carsologica Sinica* 42(4), 863–874. doi:10.11932/karst20230417

Du, J. H., Wang, Z. M., and Li, Q. M. (2010). "*Hydrocarbon exploration of carboniferous volcanic rocks in northern Xinjiang*." Beijing: Petroleum Industry Press.

Feng, J. W., Guo, H. H., Wang, R. J., Chang, L. J., Wang, C., and Gao, X. (2023). Genesis mechanism of strike -slip fracture of deep carbonate rocks in Tabei area, tarim basin. *Earth Sci.* 48, 2506–2519. doi:10.3799/dqkx.2023.110

Ford, D. C., and Williams, P. W. (2007). *Karst hydrogeology and geomorphology*. London: Unwin Hyman.

Gao, X., Ma, Q., Cao, K., Song, Q., and Dong, X. J. (2016). Characteristics and geological modeling of underground river water-eroded cave system: taking Harahatang Area of Tarim Basin as an example. *Fault-Block Oil Gas Field* 23 (6), 782–787. doi:10.6056/dkyqt201606020

Hollis, C., and Sharp, I. (2011). Albian–Cenomanian–Turonian carbonate-siliciclastic systems of the Arabian Plate: advances in diagenesis, structure and reservoir modelling: introduction. *Petroleum Geoscience* 17, 207–209. doi:10.1144/1354-079310-060

Huang, S. Y., and Song, H. R. (1997). Deep karstification of gas-oil reservoir. *Carsologica Sin*, 2–11.

Jia, C. Z. (1997). *Tectonics Characteristics and Petroleum, Tarim Basin*. Beijing. Geological Publishing House, 29–261.

Jia, C. Z., Ma, D. B., Yuan, J. Y., Wei, G. Q., Yang, M., Yan, L., et al. (2021). Structural characteristics, formation and evolution and genetic mechanisms of strizke–slip faults in the Tarim Basin. *Nat. Gas. Ind. B* 9 (1), 51–62. doi:10.1016/j.ngib.2021.08.017

Jiang, Y. B., and Li, X. J. (2021). Development model of paleokarst caves in the Middle-Lower Ordovician of TH12402 well area in Tahe oilfield, Tarim Basin. *J. Palaeogeogr.* 23 (4), 824–836. doi:10.7605/gdlxb.2021.04.044

Jin, Q., Tian, F., Lu, X. B., and Kang, X. (2015). Characteristics of collapse breccias filling in caves of runoff zone in the Ordovician karst in Tahe Oilfield, Tarim Basin. *Oil Gas Geol.* 36 (5), 729–735. doi:10.11743/ogg20150503

Klimchouk, A. (2009a). Morphogenesis of hypogenic caves. *Geomorphology* 106, 100–117. doi:10.1016/j.geomorph.2008.09.013

Klimchouk, A. (2009b). "Principal features of hypogene speleogenesis," in *Hypogene speleogenesis and karst hydrogeology of artesian basins: simferopol, Ukraine, Ukrainian Institute of Speleology and Karstology*. Editors A. B. Klimchouk, and D. C. Ford, 7–15.

Klimchouk, A., Auler, A. S., Bezarra, F. H., Cazarin, C. L., Balsamo, F., and Dublyansky, Y. (2016). Hypogenicorigin,geologic controlsandfunctional organization ofagiant cave system in Precambrian carbonates, Brazil. *Geomorphology* 253, 385–405. doi:10.1016/j.geomorph.2015.11.002

Lei, C., Chen, H. H., Su, A., and Han, S. M. (2014). Characteristics and preservation mechanism of the Ordovician deep burial karst caves in Tahe area. *Lithol. Reserv.* 26 (2), 27–31.

Li, G. H., Li, S. Y., Li, H. Y., Sun, C., Xie, Z., and Li, F. (2021). Distribution pattern and formation mechanism of the strike-slip fault system in the central Tarim Basin. *Nat. Gas. Ind.* 41 (3), 30–37. doi:10.3787/j.issn.1000-0976.2021.03.004

Li, H., Wang, G., Li, Y., Bai, M., Pang, X., Zhang, W., et al. (2023). Fault-Karst systems in the deep ordovician carbonate reservoirs in the yingshan Formation of Tahe oilfield Tarim Basin, China. *Geoenergy Sci. Eng.* 231, 212338. doi:10.1016/j.geoen.2023.212338

Li, J. (2020) "*Characteristics analysis of fracture-cavity units in ordovician carbonate fracture-cavity reservoirs in the northern Halahatang oilfield*," in Chengdu. Southwest Petroleum University.

Li, M., Tang, L., Qi, L., Huang, T., Zhen, S., and Tian, Y. (2015). Differential tectonic evolution and its controlling on hydrocarbon accumulation in the south slope of Tabei uplift. *Nat. Gas. Geosci.* 2 (26), 218–228. doi:10.11764/j.issn.1672-1926.2015.02.0218

Li, Y. (2012). *Ordovician carbonate fracture-cavity reservoirs identification and quantitative characterisation in Tahe Oilfield*. Journal of China University of Petroleum, 36, 1–7.

Lin, B., Zhang, X., Kuang, A., Yun, L., Liu, J., Li, Z., et al. (2021). Structural deformation characteristics of strike-slip faults in Tarim Basin and their hydrocarbon significance: a case study of No. 1 fault and No. 5 fault in Shunbei area. *Acta Pet. Sin.* 42 (7), 906–923. doi:10.7623/syxb202107006

Liu, Q., Zhang, Y. T., Chen, S., Song, X. G., Li, T., Kang, P. F., et al. (2023). Development and evolution characteristics of strike-slip faults in Tarim Basin and its geological significance: a case study of F_I 17 fault in Fuman Oilfield. *Geoscience* 37 (05), 1123. doi:10.19657/j.geoscience.1000-8527.2023.058

Liu, X. W., Zhu, Y. F., Su, J., Wang, K., and Zhang, B. T. (2014) "*The characteristics and the controlling accumulation factors of buried hill reservoir in hanilcatam*," in Tarim Basin: Journal of Southwest Petroleum University, 37–46.

Loucks, R. G. (1999). Paleocave carbonate reservoirs: origins, burial-depth modifications, spatial complexity, and reservoir implications. *AAPG Bulletin*, 83, 1795–1834.

Loucks, R. G., and Mescher, P. K. (2002). "Paleocave facies classification and associated pore types, in Paleo caves reservoirs: origin, spatial complexity, and reservoir implications," in *Abilene geological society*. Abilene: Texas, 1–18.

Lu, H. T., Zhang, D. J., and Yang, Y. C. (2009). Stages of paleokarstic hypergenesis in ordovician reservoir, Tahe oilfield. *Geol. Sci. Technol. Inf.* 28 (6), 71–75. doi:10.3969/j.issn.1000-7849.2009.06.011

Lu, X., Yang, M., Wang, Y., Bao, D., Cao, F., and Yang, D. (2018). Geological characteristics of "strata-bound" and fault-controlled reservoirs in the northern Tarim Basin: taking the Ordovician reservoirs in the Tahe Oil Field as an example. 40(4): 461–469.

Ma, B., Tian, W., Wu, G., Nance, R. D., Zhao, Y., Chen, Y., et al. (2022). The subduction-related great unconformity in the Tarim intracraton, NW China. *Glob. Planet. Change* 215, 103883. doi:10.1016/j.gloplacha.2022.103883

Ma, B., Wu, G., Zhang, Y., Scarselli, N., Yang, B., Jiang, Y., et al. (2024). New constraints from *in-situ* U-Pb ages and fluid inclusions of calcite cement and structural analysis on multiple stages of strike-slip fault activities in the northern Tarim Basin, NW China. *J. Asian Earth Sci.* 273, 106246. doi:10.1016/j.jseaes.2024.106246

Ma, D. B., Wu, G. H., Zhu, Y. F., Tao, X. W., Chen, L. X., Li, P. F., et al. (2019). Segmentation characteristics of deep strike-slip faults in the Tarim Basin and its control on hydrocarbon enrichment: taking the Ordovician strike-slip fault in the Halahatang Oilfield in the Tabei area as an example. *Earth Sci. Front.* 26 (1), 225–237. doi:10.13745/j.esf.sf.2019.1.10

Ma, Q. Q., and Duan, T. Z. (2023). Multi-level ultra-deep fault-controlled karst reservoirs characterization methods for the Shunbei field. *Front Earth Sci.* 11, 1149678. doi:10.3389/feart.2023.1149678

Machel, H. G., Borrero, M. L., Dembicki, E., Huebscher, H., Ping, L., and Zhao, Y., (2012). The Grosmont: the world's largest unconventional oil reservoir hosted in carbonate rocks, *Geologic. Soc.*, 370: 49–81. doi:10.1144/sp370.11

McMechan, G. A., Loucks, R. G., Mescher, P., and Zeng, X. (2002). Characterization of a coalesced, collapsed paleocave reservoir analog using GPR and well-core data. *Geophysics* 67 (4), 1148–1158. doi:10.1190/1.1500376

Miall, A. D. (1996). *The geology of fluvial deposits: case studies and modern approaches*. Berlin: Springer-Verlag.

Ning, C. Z., and Hu, S. (2020). Characterization of paleo - topography and karst caves in ordovician Lianglitage Formation, Halahatang oilfield, Tarim Basin. *Oil Gas Geol.* 41 (5), 985–996. doi:10.11743/ogg20200509

Ning, C. Z., Sun, L. D., Hu, S. Y., Xu, H., Pan, W. Q., Li, Y., et al. (2021). Karst types and characteristics of the Ordovician fracture-cavity type carbonate reservoirs in Halahatang oilfield. *Tarim. Basin* 42 (1), 15–32. doi:10.7623/syxb202101002

Onac, B. P. (2014). "Hypogene versus Epigene caves: the sulfur and oxygen isotope fingerprint," in *Hypogene cave morphologies: karst waters institute special publication*. Editors A. Klimchouk, I. Sasowsky, J. Mylroie, and S. A. Engel, 18, 1–75.

Palmer, A. N. (1991). Origin and morphology of limestone caves: geological society of America bulletin. *Geol. Soc. Am. Bull.* 103, 1–21. doi:10.1130/0016-7606(1991)103<0001:oamolc>2.3.co;2

Palmer, A. N. (2007). *Caves and karst of the USA*. Washington, 35–96.

Palmer, A. N. (2011). Distinction between epigenic and hypogenic maze caves. *Geomorphology* 134, 9–22. doi:10.1016/j.geomorph.2011.03.014

Panneerselvam, B., Pande, D., Muniraj, K., Balasubramanian, A., and Ravichandran, N. (2022). *Climate change impact on groundwater resources*. Cham: Springer. Vol. 10, 978–983.

Peng, L., Liu, X. P., Lin, C. S., Liu, J. Y., Yang, X. F., and Wang, H. P. (2009). Late Ordovician palaeogeomorphology and its sedimentary facies characteristics in central Tarim uplift. *Oil Geophys. Prospect.* 6 (4), 767–772. doi:10.1287/mksc.1080.0385

Polyak, V. J., Asmeron, Y., Hill, C. A., Palmer, A. N., Provencio, P. P., Palmer, M. V., et al. (2014). "Isotopic studies of byproducts of hypogene speleogenesis and their contribution to the geologic evolution of the western United States," in *Hypogene cave morphologies: karst waters institute special publication*. Editors A. Klimchouk, I. Sasowsky, J. Mylroie, and S. A. Engel, 18, 88–94.

Qiao, C. K. (2020). Study on karstic-fault description of ordovician Yijianfang Formation in yueman block of Halahatang Oilfield. Doctoral thesis. Beijing: China University of Petroleum.

Reading, H. G., and Richards, M. (1994) "Sedimentary environments: processes," in *Facies and stratigraphy*. Oxford: Blackwell Science.

Ren, M. E., and Liu, Z. Z. (1983). *Introduction to karstology*. Beijing: The Commercial Press, 37–125.

Shang, X. F., Duan, T. Z., Zhang, W. B., and Cheng, H. (2020). Characterization of dissolution facies belt in fracture-cavity carbonate rocks mainly controlled by fault-controlling karst: a case study of Ordovician reservoirs in the Block 10 of Tahe oilfield. *Acta Pet. Sin.* 41 (3), 329–342. doi:10.7623/syxb202003007

Shi, S. Y., Hu, S. Y., and Liu, W. (2015). Distinguishing paleokarst period by integrating carbon-oxygen isotopes and fluid inclusion characteristics. *Nat. Gas. Geosci.* 26 (2), 208–217. doi:10.11764/j.issn.1672-1926.2015.02.0208

Smith, L. B., Jr (2006). Origin and reservoir characteristics of 1111 upper ordovician trenton-black river hydrothermal 1112 dolomite reservoirs in New York: AAPG bulletin. *Am. Assoc. Pet. Geol. Bull.* 90 (11), 1691–1718. doi:10.1306/04260605078

Tang, Y., Li, M., Fang, R., Zhang, B. S., Yang, Z., He, D. X., et al. (2019). Geochemistry and origin of ordovician oils in the rewapu block of the Halahatang oilfield (NW China). *Petroleum Sci.* 16 (1), 1–13. doi:10.1007/s12182-018-0284-4

Wang, G. P., Wang, Z. L., Zhao, X. J., Li, Y. X., and Wang, N. X. (2013). Palaeogeomorphology restoring of ordovician weathering crusting yan' an area, ordos basin. *Acta Sedimentol. Sin.* 4 (31), 563–570. doi:10.14027/j.cnki.cjxb.2013.04.017

Wang, L. J. (2010). Characteristics of karst caverns in carbonate reservoir in Area 12 of Tahe Oilfield. *Inn. Mongulia Petrochem. Ind.* 36 (1), 120–122.

Wang, R. J., Wang, X., Deng, X. L., Zhang, Y. T., Yuan, J. Y., Xie, Z., et al. (2021). Control effect of strike-slip faults on carbonate reservoirs and hydrocarbon accumulation: a case study of the northern depression in the Tarim Basin. *Nat. Gas. Ind.* 41 (3), 10–20. doi:10.3787/j.issn.1000-0976.2021.03.002

Wei, W. (2018). *Development characteristics of Ordovician karst reservoir in Xinken-Rewapu block, Halahatang Oilfield*. Beijing. China University Of Petroleum.

Wu, A. M., Ma, F., Wang, G. L., Liu, J. X., Hu, Q. Y., and Miao, Q. Z. (2018a). A study of deep-seated karst geothermal reservoir exploration and huge capacity geothermal well parameters in xiongan new area. *Acta Geosci. Sin.* 39 (5), 523–532.

Wu, G., Yuan, Y., Huang, S., Thomas, M. V., Xiao, Y., Cai, Q., et al. (2018b). The dihedral angle and intersection processes of a conjugate strike-slip fault system in the Tarim Basin, NW China. *Acta Geol. Sin.* 92 (1), 74–88. doi:10.1111/1755-6724.13495

Wu, G., Kim, Y., Su, Z., Yang, P., Ma, D., and Zheng, D. (2020). Segment interaction and linkage evolution in a conjugate strike-slip fault system from the Tarim Basin, NW China. *Mar. Petroleum Geol.* 112, 104054. doi:10.1016/j.marpetgeo.2019.104054

Wu, G., Yang, H., He, S., Cao, S., Liu, X., and Jing, B. (2016). Effects of structural segmentation and faulting on carbonate reservoir properties: a case study from the Central Uplift of the Tarim Basin, China. *Mar. Petroleum Geol.* 71, 183–197. doi:10.1016/j.marpetgeo.2015.12.008

Wu, G., Yang, H., Qu, T., Li, H., Luo, C., and Li, B. (2012a). The fault system characteristics and its controlling roles on marine carbonate hydrocarbon in the Central uplift, Tarim basin. *Acta Petrol. Sin.* 28 (3), 793–805. doi:10.2110/palo.2011.p11-036r

Wu, G., Li, H., Zhang, L., Wang, C., and Zhou, B. (2012b). Reservoir-forming conditions of the ordovician weathering crust in the maigaiti slope, Tarim Basin, NW China. *Petroleum Explor. Dev.* 39 (2), 144–153.

Wu, G. H., Chen, Z. Y., Qu, T. L., Wang, C. H., Li, H. W., and Zhu, H. Y. (2012c). Characteristics of the strik-slip fault facies in ordovician carbonate in the Tarim Basin, and its relations to hydrocarbon. *Acta Geol. Sin.* 86 (2), 219–227.

Xia, R. Y., and Liang, B. (2011). *The model and genesis of Ordovician carbonate fracture-cave system in Tarim Basin*. Beijing: Geological Publishing House.

Xie, Y., Qian, P., Li, J., Yu, S., Miao, X., Guo, Y., et al. (2024). Response of weathering carbon sink effect to anthropogenic sulfuric acid in different lithological catchments: a case study from Southwest China. *J. Asian Earth Sci.* 270, 106195. doi:10.1016/j.jseaes.2024.106195

Xiong, X. J., Chen, R., Yuan, Y., Zhang, X., Feng, L., Wu, Y. H., et al. (2021). Seismic prediction of karst reservoirs of the maokou Formation in wolonghe structure of sichuan basin. *Acta Petrolei Sinica*, 42(6): 724–735.

Xu, J. H., Kang, Z. H., and Lan, Q. Q. (2022). Karst reservoir type, cave structure and genetic model of ordovician Tahe reservoirs: case study of fracture-cavity unite T615 in Tahe oilfield 7 block. *Geosciences* 34 (6), 1–13. doi:10.19657/j.geoscience.1000-8527.2020.087

Xu, Z. X., and Ma, Q. Y. (2022). Zonal differential deformation and reservoir control model of Ordovician strike-slip fault zone in Tahe Oilfield. *Mar. Orig. Pet. Geol.* 27 (2), 124–134. doi:10.3969/j.issn.1672-9854.2022.02.002

Yang, F., Liu, L. F., Ran, Q. Q., Kong, J. P., Huang, S. Q., and Huang, C. W. (2020). Characteristics of weathering crust karst reservoir of Deng 4 member in Moxi area, Sichuan Basin. *Lithol. Reserv.* 32 (2), 43–53. doi:10.12108/yxyqc.20200205

Yang, H., Zhang, Y., Guan, B., Li, F., and Cai, Q. (2023). Exploration and development of the ordovician carbonate oil field in Halahatang, Tarim Basin. *Mar. Orig. Pet. Geol.* 28 (2), 113–122. doi:10.3969/j.issn.1672-9854.2023.02.001

Yang, S., Wu, G. H., Zhu, Y. F., Zhang, Y. T., Zhao, X. X., Lu, Z. Y., et al. (2022). Key oil accumulation periods of ultra-deep fault-controlled oil reservoir in northern Tarim Basin, NW China. *Petroleum Explor. Dev.* 49 (2), 285–299. doi:10.1016/s1876-3804(22)60024-7

Yu, R. L. (2005). Characteristics and significance of the caledonian karst in the Tahe oil field, the Tarim Basin. *Petroleum Geol. Exp.* 27 (5), 468–472. doi:10.11781/sysydz200505468

Yuan, D. X. (1993). *Chinese karstology*. Beijing: Geological Publishing House, 10–15.

Zhang, H. T., Yang, M., Wang, Y., Yang, D. B., Xu, S., and Liu, J. (2021). Mechanical filling characteristics of Ordovician Karst paleo-subterranean rivers in Karst stage of Tahe oilfield. *Petroleum Geol. Eng.* 35 (6), 12–17.

Zhang, Q. (2018). *Paleokarst development mechanism of Ordovician carbonate rocks in Halahatang area*. Tarim Basin: China University of Geosciences.

Zhang, T., Yun, L., Wu, X. W., and Ye, D. S. (2005). The application of strontium isotopes in division of paleokarst stages in Tahe Oil Field. *Petroleum Geol. Exp.* 27 (3), 299–303. doi:10.11781/sysydz200503299

Zhang, Y., Sun, C., Wang, X., Yuan, J., and Yin, H. (2020a). *Reservoir Formation patterns in the strike-slip fault zone of the Halahatang oilfield*. Journal of Southwest Petroleum University, 42, 10–18.

Zhang, Y. T., Deng, X. L., Wu, G. H., Xie, Z., Wan, X. G., and Yang, T. Y. (2020b). The oil distribution and accumulation model along the strike-slip fault zones in Halahatang area, Tarim Basin. *Chin. J. Geol.* 55 (2), 382–391. doi:10.12017/dzkx.2020.025

Zhang, Z. J., Lu, Y. P., Ma, H. L., Geng, T., and Zhang, X. (2023). Fracture-cave system in collapsed underground paleo-river with subterranean flow in karst canyon area, Tahe oilfield. *Xinjiang Pet. Geol.* 44 (1), 9–17. doi:10.7657/XJPG20230102

Zhang, X. D., Jin, Q., and Zhang, S. (2022a). *Control of Ordovician fault on karst reservoirs in Tarim Basin: a case study of well block T705-S86 in Tahe oilfield*. Journal of China University of Mining and Technology, 51, 1166–1177.

Zhang, C. J., Lu, Y. P., and Zhang, Z. Z. (2022b). Features of middle-lower ordovician paleo-karst caves in western slope area, Tahe oil field, Tarim Basin. *Petroleum Geol. Exp.* 44 (6), 1008–1017. doi:10.11781/sysydz2022061008

Zhang, Z. L., Qiao, Y. P., Dou, S., Li, K. Y., Zhong, Y., Wu, L. Y., et al. (2024). Karst paleogeomorphology and reservoir control model of the 2nd member of Dengying Formation in Penglai gas area, Sichuan Basin, China. *Oil and Gas Geol.* 45 (1), 200–214. doi:10.11743/ogg20240114

Zhao, M., Qin, S., Pan, W., Song, Y., Wang, Z., Han, J., et al. (2008). The hydrocarbon source analysis of buried-hill reservoir of ordovician in western lunnan area of Tabei uplift. *Xinjiang Pet. Geol.* 29 (4), 478–481.

Zhao, X., Wu, C., Ma, B., Li, F., Xue, X., Lv, C., et al. (2023). Characteristics and genetic mechanisms of fault-controlled ultra-deep carbonate reservoirs: a case study of Ordovician reservoirs in the Tabei paleo-uplift, Tarim Basin, western China. *J. Asian Earth Sci.* 254, 105745. doi:10.1016/j.jseaes.2023.105745

Zheng, D. M., Zhang, Q. Y., Zhao, K. Z., Liang, B., Dan, Y., and Li, J. R. (2015). Ancient hydrological conditions of the Ordovician transformation zones in the Halahatang area, northern Tarim. *Carsologica Sin. (2)*, 179–186.

Zhong, L. M., Xu, M., Wu, M. L., Yang, Y. N., and Zhang, Q. (2018). Development of deep karst under the coupling of multistage flow systems: a case of southern part of the Zhongliang Mountainanticline of the parallel barrier structure in Eastern Sichuan. *Hydrogeology Eng. Geol.* 45 (1), 45–51. doi:10.16030/j.cnki.issn.1000-3665.2018.01.07

Zhu, G. Y., Yang, H. J., Zhu, Y. F., Gu, L. J., Lu, Y. H., Su, J., et al. (2011). Study on petroleum geological characteristics and accumulation of carbonate reservoirs in Hanilcatam area, Tarim basin. *Acta Petrol. Sin.* 27 (3), 827–844.

Zhu, W. P., Sun, D., Yao, Q. Z., Fang, Q. F., and Dai, D. D. (2021). The law of hydrocarbon accumulation in carbonate reservoirs in Halahatang area, Tarim Basin. *Special Oil and Gas Reservoirs* 28 (2), 41–48.

Zuo, L. Q. (2019). Review on methods of paleo-geomorphologic restoration. *Petroleum Geol. Eng.* 33 (3), 12–17.